

# Discrete influx events refill depleted $\text{Ca}^{2+}$ stores in a chick retinal neuron

Salvador Borges, Sarah Lindstrom, Cameron Walters, Ajithkumar Warriar and Martin Wilson

The depletion of ER  $\text{Ca}^{2+}$  stores, following the release of  $\text{Ca}^{2+}$  during intracellular signalling, triggers the  $\text{Ca}^{2+}$  entry across the plasma membrane known as store-operated calcium entry (SOCE). We show here that brief, local  $[\text{Ca}^{2+}]_i$  increases (motes) in the thin dendrites of cultured retinal amacrine cells derived from chick embryos represent the  $\text{Ca}^{2+}$  entry events of SOCE and are initiated by sphingosine-1-phosphate (S1P), a sphingolipid with multiple cellular signalling roles. Externally applied S1P elicits motes but not through a G protein-coupled membrane receptor. The endogenous precursor to S1P, sphingosine, also elicits motes but its action is suppressed by dimethylsphingosine (DMS), an inhibitor of sphingosine phosphorylation. DMS also suppresses motes induced by store depletion and retards the refilling of depleted stores. These effects are reversed by exogenously applied S1P. In these neurons formation of S1P is a step in the SOCE pathway that promotes  $\text{Ca}^{2+}$  entry in the form of motes.

(Received 17 August 2007; accepted after revision 15 November 2007; first published online 22 November 2007)

**Corresponding author** M. Wilson: Section of Neurobiology, Physiology and Behaviour, Division of Biological Sciences, UC Davis, Davis, CA 95616, USA. Email: mcwilson@ucdavis.edu

Calcium stored within the endoplasmic reticulum of neurons plays multiple roles in synaptic transmission and plasticity. In developing neurons,  $\text{Ca}^{2+}$  released from  $\text{Ca}^{2+}$  stores is thought to modulate the growth of dendritic processes and stabilize synapses (Lohmann *et al.* 2002, 2005; Lohmann & Wong, 2005). In mature neurons, in addition to its effects at postsynaptic sites, it is clear that  $\text{Ca}^{2+}$  released from internal stores can promote transmitter release by augmenting the  $\text{Ca}^{2+}$  entering from the extracellular medium (Llano *et al.* 2000; Emptage *et al.* 2001; Galante & Marty, 2003; Collin *et al.* 2005). This is true for retinal photoreceptors (Suryanarayanan & Slaughter, 2006), as well as the amacrine cells that are investigated in this study (Warriar *et al.* 2005). How these stores are refilled is the subject of this study.

In many non-neuronal cell types, release of  $\text{Ca}^{2+}$  from the ER is tightly coupled to a subsequent influx of  $\text{Ca}^{2+}$  across the plasma membrane, called capacitative  $\text{Ca}^{2+}$  entry (Putney, 1986) or store-operated calcium entry (SOCE), that serves both to refill the depleted internal store as well as, in many instances, to reinforce and extend the elevation of cytoplasmic  $\text{Ca}^{2+}$  concentration (Putney, 2003). Details of the mechanism by which store depletion brings about  $\text{Ca}^{2+}$  entry are unclear, although the recently identified proteins, Orai (Feske *et al.* 2006; Vig *et al.* 2006) and STIM1 (Liou *et al.* 2005; Roos *et al.* 2005) are critical components of  $\text{Ca}^{2+}$  entry through the  $I_{\text{crac}}$  channel. Orai is a novel channel protein and STIM1 is likely to

be a part of the ER  $\text{Ca}^{2+}$  sensor (Prakriya *et al.* 2006; Yeromin *et al.* 2006).  $I_{\text{crac}}$ , however, is a particular form of SOCE, characterized chiefly from lymphocytes and whose properties are not universally shared by SOCE in other cell types (reviewed in Bolotina, 2004). Consistent with this, there is some support for multiple channel types and perhaps multiple activation mechanisms mediating SOCE (Albert *et al.* 2007; Yuan *et al.* 2007).

The connection between  $\text{Ca}^{2+}$  release from the ER and subsequent  $\text{Ca}^{2+}$  entry has been less well studied in neurons than in many other cell types. SOCE, universal in non-excitable cells, was thought to be absent from excitable cells, in which voltage-gated  $\text{Ca}^{2+}$  channels (VGCCs) were supposed to refill stores. While some excitable cells do apparently lack capacitative  $\text{Ca}^{2+}$  entry (e.g. Friel & Tsien, 1992), others show store-operated  $\text{Ca}^{2+}$  currents (reviewed in Putney, 2003). It remains an open question whether, as in other cell types, store-operated  $\text{Ca}^{2+}$  influx plays any direct role in neuronal function though there are some suggestions that it might do so, for example Emptage *et al.* (2001).

In this study we examine the relationship between the state of internal  $\text{Ca}^{2+}$  stores and  $\text{Ca}^{2+}$  influx across the plasma membrane of amacrine cells derived from the embryonic chick retina. In these cells,  $\text{Ca}^{2+}$  release through  $\text{IP}_3$  receptors ( $\text{IP}_3\text{Rs}$ ) and ryanadine receptors (RyRs) can be readily triggered by the influx of  $\text{Ca}^{2+}$  through VGCCs in the plasma membrane (Hurtado *et al.* 2002) and is known

to contribute to transmitter release (Warrier *et al.* 2005). A practical advantage offered by these cells is that their narrow dendrites,  $\sim 0.5\text{--}1\ \mu\text{m}$  diameter, mean that they are essentially one dimensional and ideally suited to confocal linescan.

In this work we show that brief, local  $\text{Ca}^{2+}$  influx events are triggered by ER  $\text{Ca}^{2+}$  store depletion, but in order to demonstrate that these events are an expression of SOCE we have first shown that sphingolipids are a step in the pathway producing SOCE and provide a useful means for manipulating the frequency of events.

## Methods

### Cells

Amacrine cell cultures derived from dissociated retinas of embryonic day 8–10 chicks were grown on individual coverslips (Gleason & Wilson, 1989). Amacrine cells identified as previously described (Huba & Hofmann, 1990; Gleason *et al.* 1993), were used after 7–11 days in culture (EE 15–19). Cells were loaded for 1 h at room temperature with the AM ester of Oregon Green 488 Bapta-1-AM (OGB-1, Molecular Probes, Eugene, OR, USA) at  $5\ \mu\text{M}$  with 0.02% w/v pluronic F-127 (Molecular Probes). In many experiments the loading solution also contained  $2\ \mu\text{M}$  thapsigargin (Calbiochem, La Jolla, CA, USA) in nominally  $0\ [\text{Ca}^{2+}]$  solution. Although in many experiments, thapsigargin was subsequently removed, internal stores were unable to refill because this drug is essentially irreversible (Sagara *et al.* 1992). Coverslips were mounted in a  $40\ \mu\text{l}$  Plexiglas chamber (model RC-24, Warner Instruments, Hampden, CT, USA). External solutions were gravity fed into the chamber at a rate of  $\sim 10\ \mu\text{l s}^{-1}$  (i.e. 1 chamber volume every 4 s), though in dye washout experiments 15–20 s was required for complete dye removal. Solution changes were accomplished using the software package Tiempo (Olympus America, Melville, NY, USA), to trigger acquisition starts from the confocal software (Fluoview FV300), and Clampex 8.0 (Molecular Devices Corp., Sunnyvale, CA, USA) to provide TTL signals for solution valve operation. All experiments were done at room temperature ( $22\text{--}25^\circ\text{C}$ ).

### External solutions and drugs

External solutions used were as follows: normal: KCl ( $5.3\ \text{mM}$ ), NaCl ( $116.9\ \text{mM}$ ), TEACl ( $20\ \text{mM}$ ),  $\text{CaCl}_2$  ( $3\ \text{mM}$ ),  $\text{MgCl}_2$  ( $0.41\ \text{mM}$ ), Hepes ( $3\ \text{mM}$ ), glucose ( $5.6\ \text{mM}$ ).  $0\ [\text{Ca}^{2+}]$ : KCl ( $5.3\ \text{mM}$ ), NaCl ( $116.9\ \text{mM}$ ), TEACl ( $20\ \text{mM}$ ),  $\text{MgCl}_2$  ( $3.41\ \text{mM}$ ), Hepes ( $3\ \text{mM}$ ), glucose ( $5.6\ \text{mM}$ ). All external solutions included  $300\ \text{nM}$  TTX to suppress  $\text{Na}^+$  currents, and were adjusted for pH to 7.4 with NaOH. In those experiments employing  $\text{La}^{3+}$

or  $\text{Gd}^{3+}$ , these ions were added to the external solution without removal of  $\text{Ca}^{2+}$ .

The following drugs were obtained from Sigma (St Louis, MO, USA) and made up as stock solutions as described. AP-5, GABA, glutamate, picrotoxin,  $\text{La}^{3+}$  chloride, pertussis toxin and SKF-96365 were dissolved in water for a stock solution. Bay K8644, CNQX, MRS-1845, staurosporine and nifedipine were dissolved in DMSO for a stock solution. Sphingosine-1-phosphate, obtained as a mixture of L-threo and D-erythro forms, and sphingosylphosphorycholine (SPC) were dissolved in methanol for a stock solution. D-Sphingosine, arachidonic acid and U-73122 were dissolved in ethanol for a stock solution. Acetylcholine (ACh) and suramin were dissolved directly in the external solution.

The following drugs were obtained from Calbiochem. 2-APB, CGP-37157, ionomycin and 1-oleoyl-2-acetyl-sn-glycerol (OAG) were dissolved in DMSO for a stock solution, MLA (methyllycaconitine perchlorate) was dissolved in methanol for a stock solution. Also D-erythro-N,N-dimethyl sphingosine (DMS) from Biomol (Plymouth Meeting, PA, USA) was dissolved in ethanol for a stock solution and (RS)-2-chloro-5-hydroxyphenylglycine (CHPG) from Tocris (Ellisville, MO, USA) was dissolved in  $0.1\ \text{M}$  NaOH for a stock solution.

In experiments where a micropipette was used to puff a drug onto a dendrite, the pipette was placed several hundred micrometres away to avoid the effects of leakage from the pipette prior to puffing. Just before the 2–6 kPa puff, the pipette was quickly advanced close to the dendrite and then quickly withdrawn after the puff. Pipette movement was automated by storing the two positions on a modified Eppendorf 7171 micro-manipulator (Eppendorf, Westbury, NY, USA) triggered with a TTL pulse.

### $\text{Ca}^{2+}$ imaging and analysis

Experiments were conducted on an Olympus Fluoview FV300 inverted microscope (Olympus America, Melville, NY, USA), using a 488 nm argon laser excitation beam and a  $60\times$ , 1.4 NA oil immersion lens (Olympus America). Changes in dendritic fluorescence were recorded as a time series of linescan episodes. During slow linescans, like those illustrated in Fig. 1B and C, the scan time was typically 102 ms per line. Length of recording episode varied depending on the protocol, but was generally at least 200 s. Scan lines comprised 800 pixels typically covering a region of dendrite  $15\text{--}20\ \mu\text{m}$  long ( $0.019\text{--}0.025\ \mu\text{m}$  per pixel). In the fastest recordings, like those illustrated in Fig. 2A, B and C, a selected portion of dendrite was scanned 10 000 times per episode. Scan time was typically 3.1 ms per line giving a total of  $\sim 31\ \text{s}$  per recording

episode. Scan lines comprised 256 pixels typically covering a region of dendrite 15–20  $\mu\text{m}$  long (0.058–0.078  $\mu\text{m}$  per pixel). Empirically we found that 12 scans on the same dendrite were well tolerated but more than this tended to produce permanent damage indicated by swelling, as seen in the Nomarski image, and often a permanent increase in fluorescence. Data were rejected if the dendrite showed swelling. Control experiments showed the movement of the scan line was less than a pixel width (0.05  $\mu\text{m}$ ) over a recording episode of 31 s. Maximum deviation of the line displayed on the monitor (Fig. 1A), relative to the actual scan path was no more than 3 pixel widths.

Raw image data were exported from the FluoView software package as 16-bit single-channel TIFF files and analysed using custom coded MATLAB 6 (Mathworks, Inc., Natick, MA, USA) programs. For the fastest recordings, processing started with low-pass Gaussian filtering in the time and spatial domains to improve the low signal/noise ratio associated with imaging very small volumes. This reduced the temporal resolution to  $\sim 150$  ms and the spatial resolution to  $\sim 1$   $\mu\text{m}$ . The reduction in fluorescence due to photobleaching during a recording episode was well described as the sum of two exponentially decaying functions whose coefficients were found by fitting regions of the trace in which no  $[\text{Ca}^{2+}]$  fluctuations were seen. With the exception of a non-recoverable component that caused a one-time reduction in fluorescence of about 20%, fluorescence recovered completely between scans. No correction for background fluorescence was necessary as off-dendrite fluorescence was negligible, as was auto-fluorescence.

The final image was represented as the relative fluorescence change of OGB-1 from baseline ( $\Delta F/F_0$ ) in which  $F_0$  was determined at the beginning of each recording episode. These images were viewed in Adobe Photoshop (Adobe Systems Inc., San Jose, CA, USA) where the dynamic range of each record was matched to the colour palette.

The majority of our results are presented as relative fluorescence change since this is sufficient to show changes in the frequency of motes. Where necessary, however, we have converted raw fluorescence values to  $[\text{Ca}^{2+}]$  using eqn (1) (Tsien, 1989) in which  $K_d = 170$  nM (Molecular Probes).

$$[\text{Ca}^{2+}] = K_d \left( \frac{F - F_{\min}}{F_{\max} - F} \right) \quad (1)$$

$F_{\min}$  and  $F_{\max}$  were determined *in situ* for each dendrite thus examined.  $F_{\min}$  was determined after a 10 min washing in nominally 0  $[\text{Ca}^{2+}]$  solution. Empirically we found that  $F_{\max}$  (fluorescence at saturating  $[\text{Ca}^{2+}]$ ) could be obtained shortly after perfusion of the dendrite with a solution containing 50 mM  $\text{K}^+$  and 3 mM  $\text{Ca}^{2+}$ . Resting values for  $[\text{Ca}^{2+}]_i$ , determined in this way, were in good

agreement with those previously published for these cells (Hurtado *et al.* 2002).

A measure of the spatial extent and duration of motes was obtained from corrected images by applying a 60% threshold, discarding the lower 40% of intensity values obtained in a recording episode. An elliptical boundary was drawn around each mote to contain its visible portion and yield axes corresponding to the spatial and temporal dimensions of the mote. Motes whose extent exceeded the edges of an image were excluded from the statistical analysis.

When motes were infrequent (for example, Fig. 2A) they could be resolved and counted; however, under conditions in which the frequency of motes at a hotspot increased dramatically, it was often difficult to determine the number of motes in a burst. To circumvent this problem, mote frequency was estimated by integrating all fluorescence ( $\int \int \Delta F/F_0 \, dx, dt$ ) greater than the bleach-corrected baseline (Fig. 3A) and so we refer to mote activity, rather than mote frequency, in statistical analyses. Statistical tests were conducted using the statistical routines provided by Sigmaplot (SPSS Inc., Chicago, IL, USA). Tests of integrated fluorescence ( $\int \int \Delta F/F_0 \, dx, dt$ ) values were performed either using paired *t* tests or one-way analysis of variance (ANOVA). For an individual cell, scans for each treatment group (control, drug and wash) were pooled for the mean. Paired *t* tests or pairwise multiple comparison ANOVA (Holm–Sidak method) were then performed between treatment groups using the means for all the cells used in the experiment. Also used was the Kruskal–Wallis one-way rank-based ANOVA with differences evaluated using Dunn's multiple comparison procedure (for data in Fig. 11).

## Results

### Thapsigargin increases $[\text{Ca}^{2+}]_i$

To elicit and characterize the refilling of internal  $\text{Ca}^{2+}$  stores we began by examining the effects of thapsigargin (TG) on  $[\text{Ca}^{2+}]_i$  within the dendrites of cultured amacrine cells. By inhibiting  $\text{Ca}^{2+}$  uptake into the ER this agent depletes internal stores (Thastrup *et al.* 1990; Inesi & Sagara, 1992). In this study it serves not only to activate the  $\text{Ca}^{2+}$  influx events required for refilling but also, after prolonged treatment, to eliminate any increases in  $[\text{Ca}^{2+}]_i$  that might be caused by release of  $\text{Ca}^{2+}$  from internal stores.

Dendrites loaded with Oregon Green Bapta-1-AM (OGB) (Fig. 1A) were visualized using confocal linescan in the presence of TTX to suppress  $\text{Na}^+$  action potentials. In the nominal absence of  $\text{Ca}^{2+}$  in the bathing solution, acute application of TG (2  $\mu\text{M}$ ,  $n = 6$  cells) induced an increase in  $[\text{Ca}^{2+}]_i$  with a typical latency of approximately 40 s. After an initial rise was detected,  $[\text{Ca}^{2+}]_i$  reached a peak about

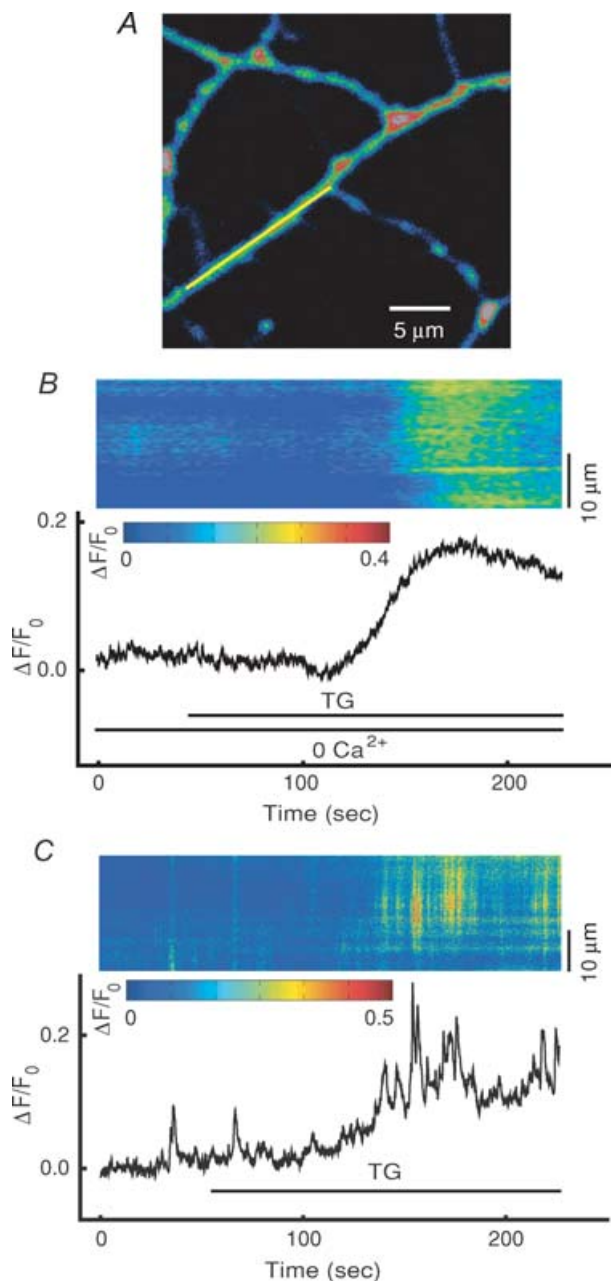


**Figure 1. Acute application of TG empties intracellular  $\text{Ca}^{2+}$  stores and increases mote production**

A, OGB-loaded amacrine dendrites in which the yellow line indicates the scan track. During slow linescans, the scan track was traversed repeatedly at 102 ms per line for several minutes resulting in a temporal representation of fluorescence change shown in B and C. During fast linescans (as in Fig. 2A), the scan track was traversed much faster at 3.1 ms per line for 10 000 repetitions. B, in this and subsequent figures, the  $\text{Ca}^{2+}$  images (top) show the bleach-corrected temporal and spatial changes in the fluorescence of the scanned dendrite. The black trace (bottom) is the spatial average of the  $\text{Ca}^{2+}$  image. Acute application of  $2 \mu\text{M}$  TG to cells in nominally 0  $[\text{Ca}^{2+}]_i$  solution produced a smooth increase in  $[\text{Ca}^{2+}]_i$  but did not induce motes. C, a similar acute application of  $2 \mu\text{M}$  TG in normal external  $[\text{Ca}^{2+}]$  solution, however, promoted an increased frequency of motes as well as a general rise in  $[\text{Ca}^{2+}]_i$ .

28–45 s later and declined to baseline within 97–210 s (Fig. 1B). This rise in  $[\text{Ca}^{2+}]_i$  reflects the emptying of ER  $\text{Ca}^{2+}$  stores as seen in other preparations (e.g. Takemura *et al.* 1989). Acute application of TG ( $2 \mu\text{M}$ ) to cells in normal external  $[\text{Ca}^{2+}]$  solution also produced a rise in  $[\text{Ca}^{2+}]_i$ , after a latency of several tens of seconds, but in addition, always produced a dramatic increase in local  $[\text{Ca}^{2+}]_i$  fluctuations ( $n = 6$ , Fig. 1C). The dependence of local  $[\text{Ca}^{2+}]_i$  fluctuations on external  $\text{Ca}^{2+}$  suggests that they are produced by a process separate from the emptying of ER  $\text{Ca}^{2+}$  stores and, as we confirm, represent  $\text{Ca}^{2+}$  influx across the plasmalemma.

### Notes

To examine  $[\text{Ca}^{2+}]_i$  fluctuations in greater detail, we took advantage of the fact that while acute application of TG produced a barrage of fluctuations (Fig. 1C), the frequency of these events always dropped over a period of minutes. Following a 1 h incubation of cells with  $2 \mu\text{M}$  TG in nominally 0  $[\text{Ca}^{2+}]$  solution and a subsequent 10 min in normal external  $[\text{Ca}^{2+}]$ , the frequency of local fluctuations was typically, when averaged over long times, one or two  $[\text{Ca}^{2+}]_i$  events during a 31 s recording episode in a 15–20  $\mu\text{m}$  long segment of dendrite. We noticed, however, that events frequently appeared in bursts with long intervening periods of quiet.

Using high speed scans, we analysed individually resolved  $[\text{Ca}^{2+}]_i$  events (Fig. 2A). Events typically spread  $\sim 8 \mu\text{m}$  ( $7.8 \pm 2.70 \mu\text{m}$ ) and had a duration of  $\sim 600$  ms ( $627 \pm 466$  ms,  $n = 28$  events from 10 cells). The large variance in the duration of events gives the somewhat misleading impression that event kinetics were highly variable. In fact, for any particular site, events had apparently similar rise and fall rates and the chief source of variation was in event amplitude. As smaller events were distinguishable from background noise for a relative brief period, the variance of duration, and to a lesser extent spatial spread, are high. In  $x-t$  plots like Fig. 2B, individual events had a curved leading edge consistent with a point origin along the dendrite. To confirm this we followed the method of Sun *et al.* (1998), transforming events so that the values of  $x$  were taken as distance from the apparent point of origin presented on a scale of distance squared. Plotted in this way the leading edges of events were well fitted with a straight line, as expected if events were due to  $\text{Ca}^{2+}$  briefly entering the cytoplasm at a point and passively diffusing in obedience to Fick's law. To simplify the text we will refer to these brief, stereotyped events as 'motes' (meaning tiny particles or specks).

To estimate the peak magnitude of motes we found  $F_{\text{max}}$  and  $F_{\text{min}}$ , as described in the Methods section, in dendrites from which motes had been recorded.

Peak  $[Ca^{2+}]_i$  values were found to lie between 132 and 280 nM with a mean of 197.4 nM ( $\pm 49.3$  nM). Resting  $[Ca^{2+}]_i$  following TG treatment was 39.7 nM ( $\pm 17.8$  nM,  $n = 7$  cells), in good agreement with the value of 35 nM

found using ratiometric imaging with Fura-2 (Hurtado *et al.* 2002).

In order to decide whether the chaotic barrage of fluctuations seen shortly after the application of TG (as in

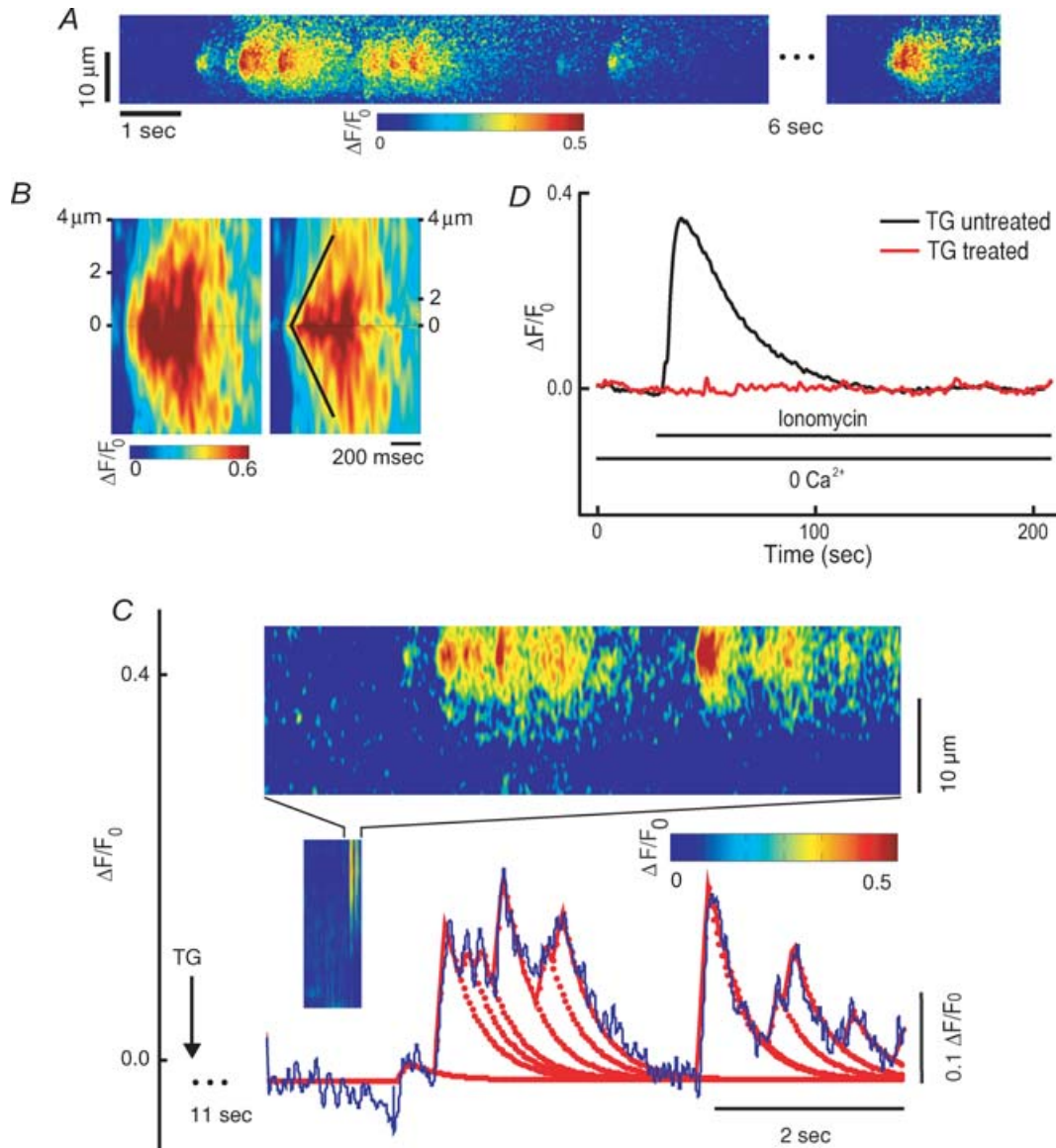


**Figure 2. Motes are discrete  $Ca^{2+}$  events that originate from a point source and persist when intracellular  $Ca^{2+}$  stores are completely emptied by TG**

*A*, a fast linescan showing an example of motes originating from a hotspot in a store-depleted dendrite. *B*, left: an individual mote scanned at a resolution of 3.1 ms per line and  $0.058 \mu\text{m}$  per pixel showing the spread of  $Ca^{2+}$ . Right: the same mote transformed so that the vertical axis is proportional to distance squared. From Fick's law,  $Ca^{2+}$  is expected to spread linearly on this transformed scale. Diagonal lines are good fits to the iso-fluorescence edges of diffusing  $Ca^{2+}$ . *C*, inset: a 31 s fast linescan compressed to have the same temporal resolution as Fig. 1C. The acute application of TG produces rapid fluctuations that, when viewed on a fast timescale (top), are seen to comprise multiple motes. Bottom: the spatial average of  $\Delta F/F_0$  (blue) shows TG-induced motes fitted with an elementary template function (red), that rises linearly with time then falls exponentially with  $\tau = 300$  ms. By scaling only the template amplitude and adjusting arrival times, the profile of fluorescence change is well fitted. *D*, typically, the bath application of ionomycin ( $10 \mu\text{M}$ ) in  $0 [Ca^{2+}]_o$  external solution results in a release of  $Ca^{2+}$  from internal stores (black). In a TG-treated dendrite, bath application of ionomycin ( $10 \mu\text{M}$ ) in  $0 [Ca^{2+}]_o$  external solution does not increase  $[Ca^{2+}]_i$  (red). This indicates that internal  $Ca^{2+}$  stores have been depleted by the TG pretreatment.

Fig. 1C), is composed of the same motes seen at relatively long times after the application of TG, we performed high speed scans shortly after the application of TG. Since  $F_0$  was determined at the beginning of each 31 s scan period, this approach necessarily removed information about the slow change in  $[Ca^{2+}]_i$  but it did permit good resolution of fluctuations. As shown in Fig. 2C it is clear that the chaotic fluctuations seen at slow scan speed are actually bursts of motes of normal dimensions. We go on to show that motes are discrete influx events associated with SOCE and we attribute the slowdown in mote frequency to the  $Ca^{2+}$ -dependent inactivation that has been described both for SOCE mediated by  $I_{crac}$  (Zweifach & Lewis, 1995; Parekh, 1998) as well as in  $Ca^{2+}$  entry by apparently non- $I_{crac}$  SOCE (Singh *et al.* 2002).

### Motes reflect $Ca^{2+}$ influx across the plasmalemma

Brief, local  $[Ca^{2+}]_i$  events due to  $Ca^{2+}$  release from the ER, called puffs (Yao *et al.* 1995) when originating from  $IP_3$ Rs, and sparks when originating from RyRs (Cheng *et al.* 1996), have been widely reported in neurons, for example, in chick embryonic ganglion cells (Lohmann *et al.* 2002, 2005), in hippocampal neurons and PC12 cells (Koizumi *et al.* 1999). Motes, however, are not due to release of  $Ca^{2+}$  from internal stores but depend instead on entry from the external medium. This conclusion is supported by several lines of evidence, the first of which is that motes are seen after prolonged treatment with TG that results in the complete and permanent emptying of stores (e.g. Fig. 2A).

Confirmation that stores were indeed permanently depleted was provided by experiments in which neurons were incubated for 1 h with  $2 \mu M$  TG in nominally  $0 [Ca^{2+}]$  solution and subsequently returned to normal external  $[Ca^{2+}]$  for at least 10 min. Dendrites were imaged while either  $20 mM$  caffeine ( $n = 6$  cells) or  $10 \mu M$  ionomycin, a  $Ca^{2+}$  ionophore, was applied in the absence of external  $Ca^{2+}$  (Fig. 2D,  $n = 5$  cells). In agreement with Hurtado *et al.* (2002), who used thimerosal, a reagent that also promotes  $Ca^{2+}$  efflux from internal stores, we found that no rise in  $[Ca^{2+}]_i$  occurred after TG treatment although strong increases were elicited in cells without prior TG treatment. These results imply that stores were unable to refill and that TG-resistant stores are not found in dendrites of these cells. As prior treatment with TG rules out the possibility that fluctuations could be puffs or sparks, we have conducted many of the subsequent experiments on cells treated in this way (subsequently called 'store-depleted cells').

From the foregoing experiments it seems likely that motes are the result of  $Ca^{2+}$  entry from the external medium. This supposition was confirmed in experiments on store-depleted cells in which normal external solution

was quickly replaced with a nominally  $0 [Ca^{2+}]$  solution. As shown in Fig. 3A, removal of external  $Ca^{2+}$  produced a complete cessation of mote activity. This treatment was effective at suppressing motes within only a few seconds – no longer than the time required for a complete change of the bathing solution. In order to quantify this change in mote frequency but avoid the uncertainties associated with counting motes, we adopted an indirect measure of frequency (see Methods) that uses the fact that motes represent the only transient increases in  $[Ca^{2+}]_i$  seen in these dendrites. As illustrated in Fig. 3A, we integrated fluorescence ( $\Delta F/F_0$ ) records along both the  $x$  and  $t$  axes, thus yielding a single unitless number representing the mote activity for each trace. Typically, the integrals from 3 to 5 fast linescan episodes of 31 s duration each, were averaged together in control conditions, in drug, and in the subsequent wash, thereby allowing statistical comparisons. Expressed in this way, the reduction in mote activity upon external  $Ca^{2+}$  removal (Fig. 3B) is highly significant (control  $172.5 \pm 15.7$ ,  $0 [Ca^{2+}]$   $13.2 \pm 8.6$ , wash  $186.3 \pm 10.2$ ,  $n = 5$  cells,  $t$  test  $P < 0.001$ ).  $La^{3+}$  ions, externally applied, also caused rapid abolition of motes. At  $25 \mu M$ ,  $La^{3+}$  suppressed all store-depleted motes with a latency of only a few seconds (control  $172.7 \pm 13.8$ ,  $La^{3+}$   $6.3 \pm 6.9$ , wash  $165.5 \pm 10.1$ ,  $n = 6$  cells,  $t$  test  $P < 0.001$ , Fig. 3C) and in a few experiments we found that lower concentrations ( $1 \mu M$ ) were also effective, but had a longer latency.

### Motes are not produced by neurotransmitter- or voltage-gated channels

We considered the possibility that motes represent  $Ca^{2+}$  entry through a cluster of postsynaptic receptors gated by a quantum of transmitter. A variation on this possibility is that VGCCs might be activated by local postsynaptic depolarization. Both of these mechanisms have been proposed in dendrites (Koizumi *et al.* 1999; Lohmann *et al.* 2002, 2005).

To examine the possibility that neurotransmitter-gated channels might be involved in the generation of motes, we monitored mote activity in store-depleted cells during the application of candidate transmitters and their antagonists. We examined the chief neurotransmitters shown to trigger  $Ca^{2+}$  influx: GABA (Connor *et al.* 1987; Segal, 1993; Lohmann *et al.* 2005), glutamate (Reichling & MacDermott, 1993; Dailey & Smith, 1994) and ACh (Khiroug *et al.* 1997). As shown in Table 1, none of the agents used had any effect on mote activity.

It is clear that these particular neurotransmitters do not generate motes, but rather than test all possible neurotransmitters, we suppressed voltage-gated  $Ca^{2+}$  channels. Dihydropyridine-sensitive L-type  $Ca^{2+}$  channels constitute the major voltage-gated pathway for  $Ca^{2+}$  influx

into these cells and are involved in transmitter release (Gleason *et al.* 1993, 1994; Sosa *et al.* 2002; Sosa & Gleason, 2004). Nifedipine ( $20 \mu\text{M}$ ), which is an effective  $\text{Ca}^{2+}$  channel blocker in these cells, failed to affect motes in any of five store-depleted cells examined (Table 1). Similarly,

Bay K8444 at  $6 \mu\text{M}$ , which has been shown to enhance  $\text{Ca}^{2+}$  current and transmitter release in these cells (Gleason *et al.* 1994), was also without effect.

These results demonstrate that transmitter release is unlikely to be implicated in the generation of motes,

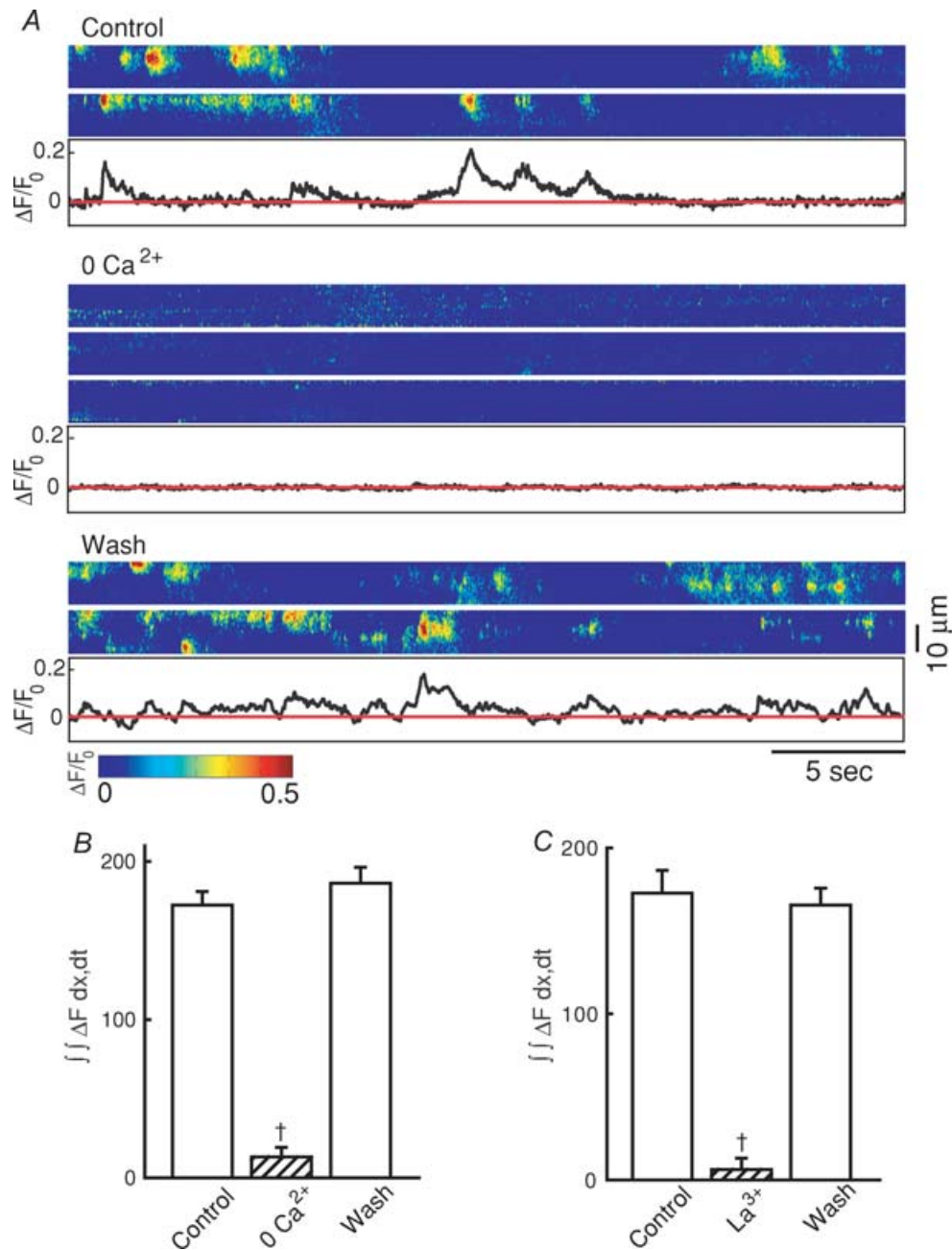


**Figure 3. Motes in store-depleted cells result from  $\text{Ca}^{2+}$  entry through a plasma membrane channel**

A, a series of fast linescans showing that reducing external  $[\text{Ca}^{2+}]$  to zero, eliminated mote activity in a cell with high initial mote activity. This effect was reversed by returning external  $[\text{Ca}^{2+}]$  to its normal value. Linescan records represent  $\Delta F/F_0$  obtained in multiple 31 s episodes separated by intervals of, typically, 15 s. Black traces show the spatial average of the last displayed linescan episode. Red traces show the bleach-corrected baseline. B, mote frequency was estimated by integrating all fluorescence change ( $\int \int \Delta F/F_0 dx, dt$ ) greater than the bleach-corrected baseline, showing that the effect of 0  $[\text{Ca}^{2+}]$  was statistically significant ( $n = 5$  cells) and reversible compared with controls. C,  $25 \mu\text{M}$   $\text{La}^{3+}$  in the external solution eliminated mote activity in 6 store-depleted cells. † $P \leq 0.001$ , paired  $t$  test.

**Table 1. Effects of neurotransmitters and Ca<sup>2+</sup> channel blockers**

Target	Drug (concentration)	Number of cells	Mote activity $\int \int \Delta F/F_0 dx, dt (\pm s.d.)$			Significance
			Control	Drug	Wash	
GABA <sub>A</sub> receptor	GABA (40 $\mu$ M)	6	190.2 $\pm$ 13.9	181.0 $\pm$ 16.8	183.0 $\pm$ 17.2	ns
NMDA receptor	AP-5 (25 $\mu$ M)	6	176.5 $\pm$ 22.5	169.3 $\pm$ 23.5	164.5 $\pm$ 22.2	ns
AMPA receptor	CNQX (40 $\mu$ M)	4	165.7 $\pm$ 23.0	158.9 $\pm$ 24.3	145.3 $\pm$ 28.2	ns
ACh receptor	ACh (10 $\mu$ M)	4	136.9 $\pm$ 22.6	152.7 $\pm$ 29.5	145.0 $\pm$ 22.7	ns
ACh receptor	MLA (10 $\mu$ M)	10	154.9 $\pm$ 25.8	162.6 $\pm$ 29.5	144.0 $\pm$ 27.3	ns
Ca <sup>2+</sup> channel	Nifedipine (20 $\mu$ M)	5	155.7 $\pm$ 8.9	151.2 $\pm$ 15.4	167.9 $\pm$ 23.6	ns
Ca <sup>2+</sup> channel	Bay K8444 (6 $\mu$ M)	5	170.8 $\pm$ 17.6	166.9 $\pm$ 27.6	174.1 $\pm$ 24.2	ns

Experiments were conducted on store-depleted cells. ns, not significant.

consistent with our observation that motes do not obviously originate at the intersections of dendrites. These results argue also that VGCCs are unlikely to play a direct role in admitting the Ca<sup>2+</sup> that gives rise to motes.

Additional support for this latter point was provided by the observation that motes persist in cells that were voltage clamped in whole-cell patch clamp at  $-70$  mV (data not shown), a voltage negative to the activation range for Ca<sup>2+</sup> current in these cells (Gleason *et al.* 1993, 1994).

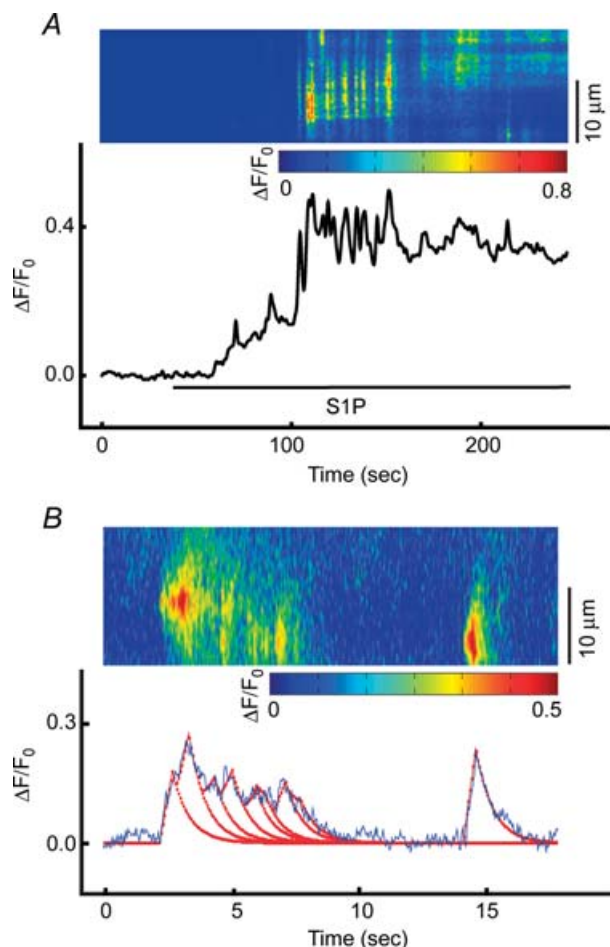


**Figure 4. S1P increases [Ca<sup>2+</sup>]<sub>i</sub> and the production of motes in store-depleted cells**

*A*, a typical slow linescan showing that S1P (10  $\mu$ M) applied to a store-depleted cell in normal external [Ca<sup>2+</sup>] induced a sustained increase of [Ca<sup>2+</sup>]<sub>i</sub>, accompanied by an increased production of motes. *B*, when examined on a fast timescale, motes evoked by application of S1P are seen to comprise multiple motes of normal dimensions. As in Fig. 2C, an elementary template function (red) has been fitted to the data.

### Sphingolipids control mote activity

Before describing experiments in which we further examine the relationship between motes and internal Ca<sup>2+</sup> stores, we first show that sphingolipids provide useful tools for manipulating mote frequency and are a step in the pathway coupling store depletion to Ca<sup>2+</sup> influx.

Sphingosine-1-phosphate (S1P) at 10  $\mu$ M has been shown to promote Ca<sup>2+</sup> influx linked to SOCE in HL60 cells and human neutrophils (Itagaki & Hauser, 2003). We therefore examined its effect on store-depleted amacrine cells. S1P at 10  $\mu$ M had, following a delay of about 1 min, two effects on [Ca<sup>2+</sup>]<sub>i</sub>: it brought a small, sustained, though variable, rise in [Ca<sup>2+</sup>]<sub>i</sub> and also a dramatic, robust and repeatable increase in mote activity (Fig. 4A). Typically, as with the acute application of TG, motes occurred in bursts that were resolvable as individual events only in fast scans (Fig. 4B).

S1P approximately doubled mote activity on average (Fig. 5A and C; Table 2). We found similar increases with the precursor to S1P, D-sphingosine (Sph) at 10  $\mu$ M except that this agent acted after a delay of several minutes (Fig. 5B and D; Table 2). Sphingosylphosphorylcholine (SPC, 10  $\mu$ M), structurally similar to S1P, also increased mote activity (Table 2). When 25  $\mu$ M La<sup>3+</sup> was applied in the presence of S1P, motes were abolished (Fig. 6A; Table 2). Similarly, application of S1P in nominally 0 [Ca<sup>2+</sup>] solution elicited no motes until normal external [Ca<sup>2+</sup>] was restored (data not shown).

We examined the question of whether S1P induces motes at novel sites along the dendrite, or alternatively whether it increases the frequency only at pre-existing sites. Motes in store-depleted cells were observed in three to four scan episodes of 31 s duration prior to the application of S1P. Of the dendritic segments (15.6–21.6  $\mu$ m in length) from 23 cells examined, mote-generating sites, or hotspots, were readily identifiable and generally numbered between



**Table 2. Effects of sphingolipids**

Drug 1 (concentration)	Mote activity $\int \int \Delta F/F_0 \, dx, dt$ ( $\pm$ s.d.)			
	Control	Drug 1	Drug 1 + Drug 2	Wash
S1P (10 $\mu$ M)	118.3 $\pm$ 13.8	228.0 $\pm$ 50.5 $\dagger\dagger$	—	117.6 $\pm$ 5.2
Sph (10 $\mu$ M)	120.8 $\pm$ 34.5	242.1 $\pm$ 90.8 $\dagger$	—	114.9 $\pm$ 20.4
SPC (10 $\mu$ M)	142.7 $\pm$ 12.5	268.7 $\pm$ 38.7 $\dagger\dagger$	—	163.6 $\pm$ 34.8
S1P (10 $\mu$ M)	151.6 $\pm$ 16.0	311.9 $\pm$ 30.6**	+La <sup>3+</sup> (25 $\mu$ M) 12.6 $\pm$ 7.4*	161.7 $\pm$ 15.6
DMS (7 $\mu$ M)	170.5 $\pm$ 14.6	19.1 $\pm$ 4.6**	+Sph (10 $\mu$ M) 17.0 $\pm$ 4.1**	153.2 $\pm$ 6.3
DMS (10 $\mu$ M)	168.2 $\pm$ 18.0	13.4 $\pm$ 12.6*	+S1P (10 $\mu$ M) 278.6 $\pm$ 20.3*	168.5 $\pm$ 22.7

Experiments were conducted on store-depleted cells.  $n = 5$  cells in each group. Statistical comparisons are relative to control.  $t$  test:  $\dagger\dagger P \leq 0.001$ ,  $\dagger P \leq 0.003$ , ANOVA: \*\* $P \leq 0.01$ , \* $P \leq 0.025$ .

one and three. After addition of S1P it was clear that the overwhelming majority of all the increased activity occurred at previously identified hotspots; in fact only 13% of the hotspots identified in the presence of S1P were novel (Fig. 6B). Very probably a longer period of observation before the application of S1P would have

decreased this percentage. Virtually all hotspots showed an increased frequency in the presence of S1P. These observations make it clear that S1P can act only at a limited number of stationary sites in a dendrite. Furthermore, they rule out the possibility that S1P is acting in a random and non-specific manner by, for instance, inducing pore

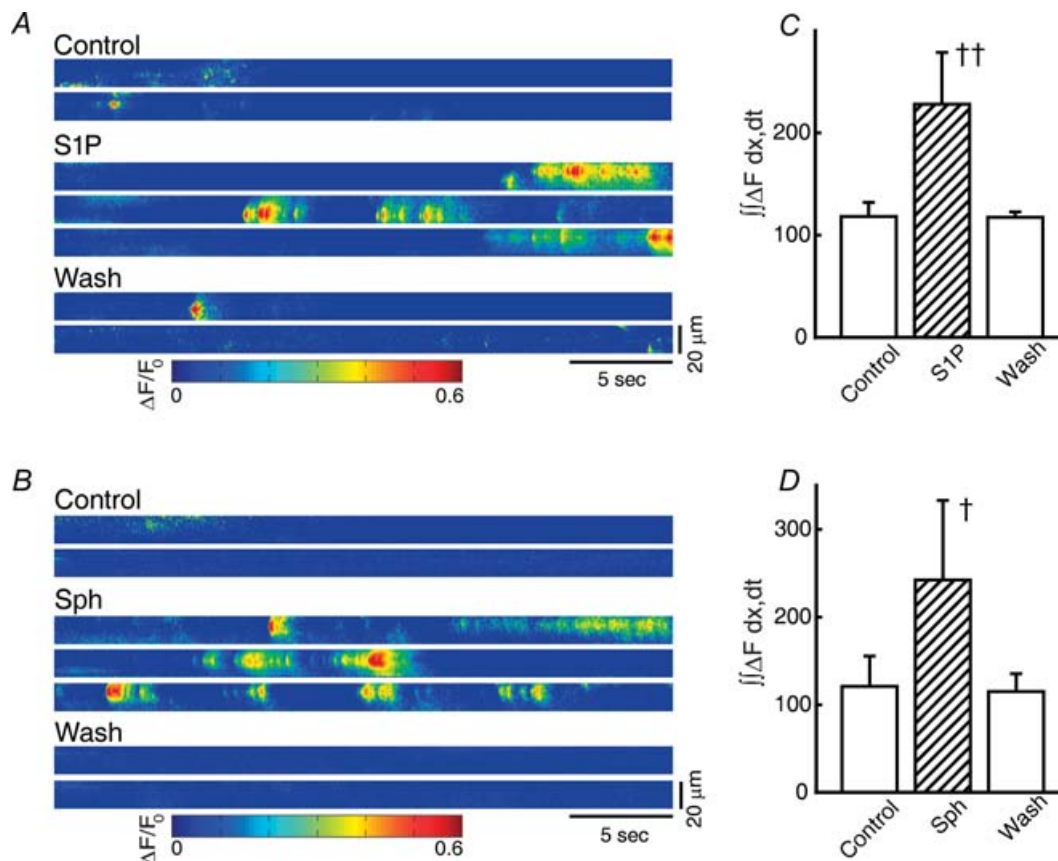


**Figure 5. Spingosine and related lipids increase the activity of motes in store-depleted cells**

A and B, fast linescan images showing the increase in mote activity associated with application of S1P (10  $\mu$ M) and Sph (10  $\mu$ M), respectively. Normal external or drug solutions were exchanged for at least 30 s before data acquisition began. Solution flow was stopped during data acquisition. Each dendrite was scanned in 3, 31 s episodes in normal external solution, 3–5 episodes in drug, and 3–4 episodes after washing the drug off with normal external solution. C and D, summary of the effects on mote activity associated with application of S1P and Sph ( $\dagger P \leq 0.003$ ,  $\dagger\dagger P \leq 0.001$ , paired  $t$  test).

formation in the plasma membrane. In a few experiments we scanned the edges of cell bodies and were able to establish that mote hotspots are not confined to dendrites (data not shown).

*N,N*-dimethylsphingosine (DMS) is a competitive inhibitor with a  $K_i$  of 2–5  $\mu\text{M}$  for sphingosine kinase, the enzyme responsible for the *in vivo* synthesis of S1P (Yatomi *et al.* 1996; Edsall *et al.* 1998). We applied DMS at concentrations of 2.5–10  $\mu\text{M}$  to dendrites of store-depleted cells. At these concentrations, an almost complete but reversible cessation of mote activity was seen (Fig. 7A). However, in the case of 2.5  $\mu\text{M}$  DMS, a latency of about 5 min separated the introduction of the inhibitor and the cessation of activity. DMS (7  $\mu\text{M}$ ) suppressed the increase in mote activity when co-applied with Sph (Fig. 7B, Table 2) but, even 10  $\mu\text{M}$  DMS, was unable to suppress the activity increase when co-applied with S1P (10  $\mu\text{M}$ ) (Fig. 7C, Table 2). These results suggest that it is the kinase product, S1P, rather than its substrate, Sph, that is the active agent promoting mote activity.

A possible concern with the experiments using DMS is that it might not be acting solely on sphingosine kinase. In particular, it has been reported that DMS inhibits PKC (Igarashi *et al.* 1989; Yang *et al.* 1999), though other studies do not support this (Edsall *et al.* 1998). To investigate the possible role of PKC we examined store-depleted cells for the effects of staurosporine (20 nM), an inhibitor for protein kinases, but not sphingosine kinase (Yang *et al.* 1999). Staurosporine had no effect on motes nor did it prevent the increase in mote activity with S1P (Fig. 7D, Table 3)

Application of S1P, Sph or SPC, to a variable degree, induced a slow, sustained rise in  $[\text{Ca}^{2+}]_i$  upon which motes rode (Fig. 4A; mean sustained  $[\text{Ca}^{2+}]_i$ ,  $125.8 \pm 27.2$  nM from six cells to which S1P was applied). As with motes themselves (Fig. 6A), 25  $\mu\text{M}$   $\text{La}^{3+}$  rapidly abolished this sustained rise in  $[\text{Ca}^{2+}]_i$  ( $n = 5$  cells; data not shown); nevertheless an obvious possibility is that motes are

triggered by this sustained increase. To examine this possibility we induced similar increases in  $[\text{Ca}^{2+}]_i$  through the application of ionomycin at 10  $\mu\text{M}$  to store-depleted cells in the presence of normal external  $[\text{Ca}^{2+}]_o$ . As shown in the slow scan of Fig. 8A, this treatment did increase  $[\text{Ca}^{2+}]_i$  ( $139.2 \pm 14.3$  nM in 5 cells) but never increased mote activity (Table 3). From this we conclude that the sustained increase in  $[\text{Ca}^{2+}]_i$  is not the cause of motes, but might instead be the consequence of increased mote activity, for example if  $\text{Ca}^{2+}$  from motes was accumulating. Two further observations suggest that the channels responsible for motes are also responsible for the sustained rise in  $[\text{Ca}^{2+}]_i$ . First, DMS not only abolished motes induced by the application of Sph, but also abolished the sustained rise in  $[\text{Ca}^{2+}]_i$  ( $n = 5$  cells; data not shown). Second, careful analysis of records like that in Fig. 4A, showed that the sustained rise in  $[\text{Ca}^{2+}]_i$  was greatest at the site of mote production and fell off by 50% at  $\sim 5.4$   $\mu\text{m}$  away from this location (Fig. 8B).

### S1P does not work through a G protein

The fact that motes are seen in cells whose  $\text{Ca}^{2+}$  stores have been emptied with TG, precludes the interpretation that they are the result of S1P acting at an S1P receptor on the plasma membrane, and thereby promoting release of  $\text{Ca}^{2+}$  from internal stores. It does not, however, preclude the possibility that S1P acts at an S1P receptor on the plasma membrane that in turn leads to the gating of a plasma membrane  $\text{Ca}^{2+}$  channel. The long lasting nature of the effect of S1P (at least 5 min in our experiments) in raising the activity of motes seems unlike the effects described for S1P receptors which are known to desensitize quickly (van Koppen *et al.* 1996; Meyer zu Heringdorf *et al.* 2003). To examine this question directly we applied agents likely to interfere with G protein-mediated pathways.

The receptors for S1P,  $\text{S1P}_{1-5}$ , are all able to signal via the pertussis toxin (PTX)-sensitive  $\text{G}_i$  (Spiegel & Milstien,

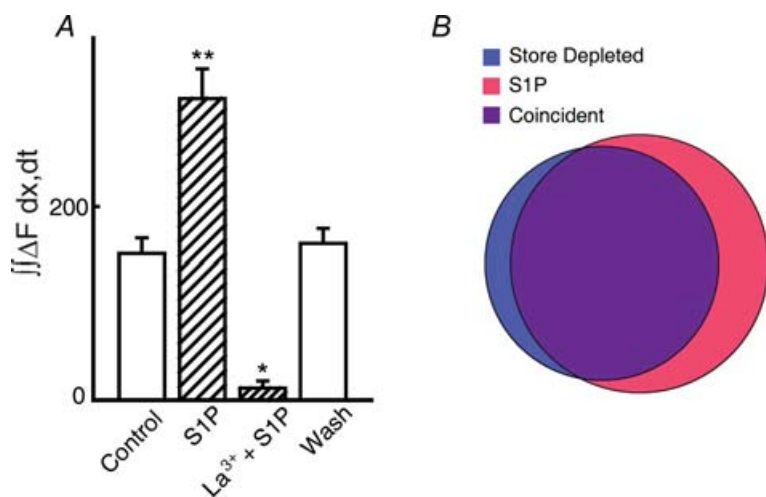


**Figure 6. Motes elicited by S1P are blocked by  $\text{La}^{3+}$  and occur at the same dendritic locations identified before S1P application**

A, motes elicited with S1P in store-depleted cells are suppressed in 25  $\mu\text{M}$   $\text{La}^{3+}$  ( $*P \leq 0.025$ ,  $**P \leq 0.01$ , ANOVA, Table 2). B, a Venn diagram summarizing the number of hotspots seen in 23 store-depleted cells. Most hotspots were active both prior to and during S1P application; 87% of the hotspots identified during the application of S1P were at locations identified as hotspots in the period prior to S1P application. Conversely, 73% of the sites identified prior to S1P application were also active in S1P.

2000; Toman & Spiegel, 2002; Sanchez & Hla, 2004) as are the more distantly related lysophospholipid receptors for which S1P is the putative natural ligand – GPR3, 6, 12 (Uhlenbrock *et al.* 2002; Ignatov *et al.* 2003) and GPR63 (Niedernberg *et al.* 2003). Cells incubated in  $1 \mu\text{g ml}^{-1}$  PTX, co-applied with TG for 1 h (Fig. 8D) were seen to have motes as usual when examined in normal external solution more than 10 min later. They also showed an increase in mote activity with applied S1P (Table 3). S1P<sub>2</sub> and S1P<sub>3</sub> are thought to be able to couple to G<sub>q</sub> and thereby activate phospholipase C (Sanchez & Hla, 2004). To eliminate the possibility that S1P was acting through this pathway we applied the PLC inhibitor U-73122 at  $20 \mu\text{M}$  for 5 min

prior to the application of S1P. This concentration of inhibitor has been shown to eliminate  $[\text{Ca}^{2+}]_i$  responses induced by the application of the peptide modulator, neurotensin, to these cells (Borges *et al.* 1996). U-73122 had no effect on the activity of motes in store-depleted cells or the mote activity seen in S1P (Fig. 8E, Table 3).

The lack of effect of U-73122 indicates that motes do not represent a  $\text{Ca}^{2+}$  entry pathway gated by diacylglycerol (DAG), or by arachidonic acid that, in other cell types, constitutes a  $\text{Ca}^{2+}$  entry pathway parallel and antagonistic to SOCE (Luo *et al.* 2001; Mignen *et al.* 2001, 2003; Moneer & Taylor, 2002; Moneer *et al.* 2003; Holmes *et al.* 2006).

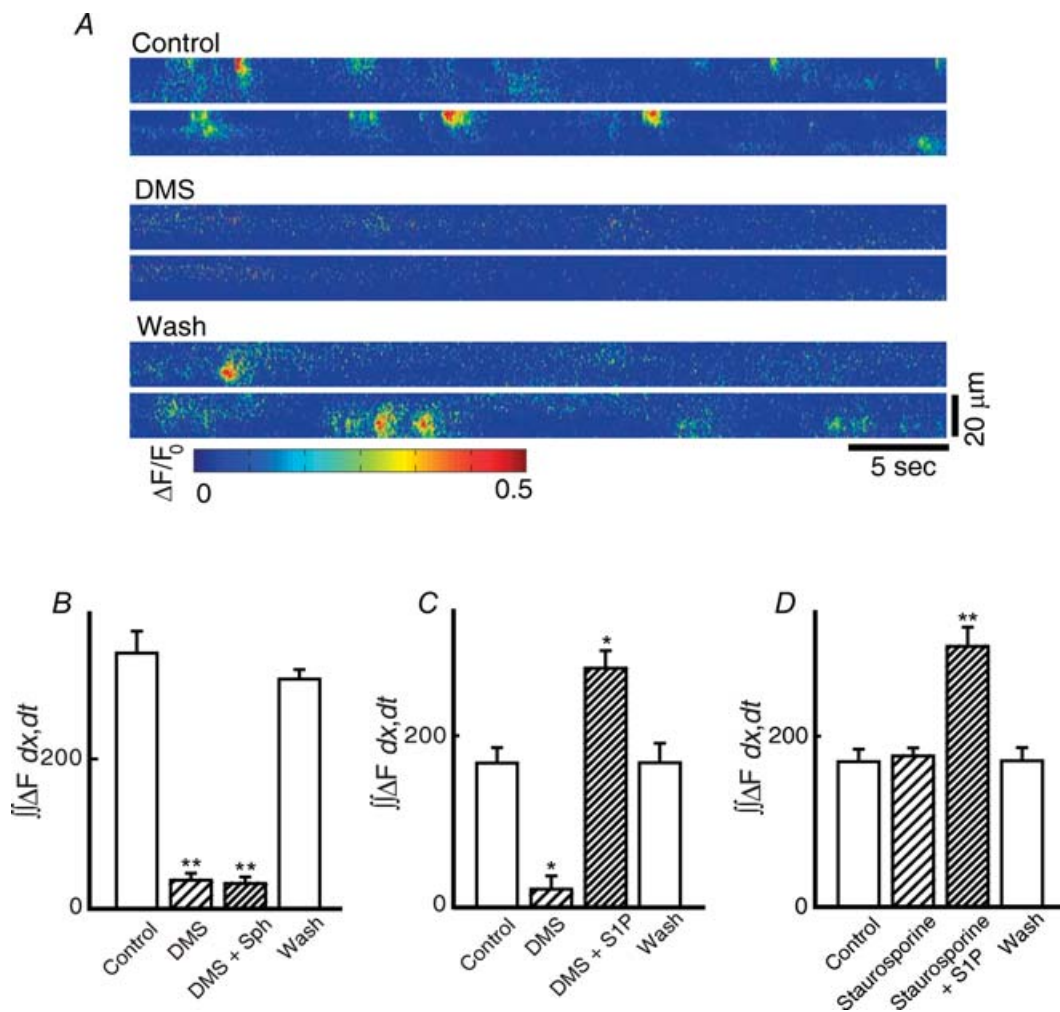


**Figure 7. DMS, a competitive inhibitor for sphingosine kinase, suppressed motes seen in store-depleted cells**

A, after several episodes of fast linescan on a cell with high initial mote activity in control solution. DMS was bath applied at  $2.5 \mu\text{M}$ . Middle records show that mote activity was eliminated entirely approximately 5 min following DMS application but recovered to normal levels when washed out (Wash). B, when  $2.5\text{--}10 \mu\text{M}$  DMS was co-applied with Sph, mote activity was suppressed ( $n = 5$  cells). C, DMS was, however, unable to suppress the increase in mote activity induced by S1P ( $n = 5$  cells). D, application of staurosporine ( $20 \text{ nM}$ ), a general protein kinase inhibitor, did not affect mote activity or suppress the increase in mote activity when co-applied with S1P ( $n = 5$  cells). \* $P \leq 0.025$ , ANOVA, \*\* $P \leq 0.01$ , ANOVA, Table 3.

**Table 3. Effects of protein kinase inhibitors and agents that affect G protein-mediated pathways and store-operated channels (SOC)**

Drug 1 (concentration)	Number of cells	Mote activity $\int \Delta F/F_0 dx, dt$ ( $\pm$ s.d.)			
		Control	Drug 1	Drug 1 + Drug 2	Wash
Staurosporine (20 nM)	5	170.3 $\pm$ 14.5	177.0 $\pm$ 9.5	+S1P (10 $\mu$ M) 305.5 $\pm$ 22.4**	171.1 $\pm$ 15.6
Ionomycin (10 $\mu$ M)	4	166.2 $\pm$ 17.3	157.4 $\pm$ 16.4	—	153.3 $\pm$ 23.0
PTX (1 $\mu$ g ml <sup>-1</sup> )	5	148.6 $\pm$ 14.2	136.6 $\pm$ 7.2	+S1P (10 $\mu$ M) 278.2 $\pm$ 22.4**	163.8 $\pm$ 20.6
U-73122 (20 $\mu$ M)	5	159.8 $\pm$ 14.2	158.5 $\pm$ 6.9	+S1P (10 $\mu$ M) 328.5 $\pm$ 8.4*	141.5 $\pm$ 14.6
AA (8 $\mu$ M)	6	158.5 $\pm$ 13.7	167.2 $\pm$ 9.5	—	177.5 $\pm$ 12.2
OAG (100 $\mu$ M)	10	141.1 $\pm$ 9.2	155.0 $\pm$ 16.7	—	177.2 $\pm$ 32.1
Suramin (100 $\mu$ M)	5	144.9 $\pm$ 8.5	151.2 $\pm$ 21.4	—	161.0 $\pm$ 27.5
S1P (10 $\mu$ M)	5	150.9 $\pm$ 8.3	249.5 $\pm$ 25.0**	+Suramin (100 $\mu$ M) 246.4 $\pm$ 26.9**	164.5 $\pm$ 27.5
SKF-96365 (20 $\mu$ M)	10	156.6 $\pm$ 7.2	163.0 $\pm$ 11.1	—	160.0 $\pm$ 7.5
MRS-1845 (10 $\mu$ M)	5	170.8 $\pm$ 17.6	166.9 $\pm$ 27.6	—	174.1 $\pm$ 24.2
2-APB (50 $\mu$ M)	5	160.7 $\pm$ 25.9	167.0 $\pm$ 23.2	—	175.6 $\pm$ 28.6
2-APB (200 $\mu$ M)	6	175.4 $\pm$ 26.4	69.2 $\pm$ 13.2†	—	187.5 $\pm$ 8.8
S1P (10 $\mu$ M)	7	161.9 $\pm$ 9.2	316.3 $\pm$ 15.2**	+2-APB (200 $\mu$ M) 69.7 $\pm$ 8.1*	173.1 $\pm$ 17.8

Experiments were conducted on store-depleted cells. Statistical comparisons are relative to control. *t* test: †*P*  $\leq$  0.003, ANOVA: \*\**P*  $\leq$  0.01, \**P*  $\leq$  0.025.

Further evidence against motes as the expression of receptor-mediated influx derives from experiments in which arachidonic acid (AA) was applied directly to store-depleted cells. AA, at a concentration that saturates this pathway (8  $\mu$ M) (Shuttleworth & Thompson, 1999), does not elicit increased mote activity (Table 3). However, as shown in Fig. 8C it does cause a general increase in  $[Ca^{2+}]_i$ . Similarly, OAG, a synthetic analogue of DAG and a well known PKC activator, was without effect on mote activity in 10 cells to which it was applied at 100  $\mu$ M (Table 3).

Suramin is an anionic polycyclic known to interfere with G protein-coupled pathways in several ways (Freissmuth *et al.* 1999), including reducing the interaction of G- $\alpha$  subunits with their coupled receptors (Lehmann *et al.* 2002). Suramin is effective against S1P<sub>3</sub> (EDG-3) (Ancellin & Hla, 1999) and enhances the effects of S1P at GPR3, GPR6 and GPR12 (Uhlenbrock *et al.* 2002). However, in our experiments, suramin (100  $\mu$ M) was without effect on mote activity in store-depleted cells (Table 3); nor did it inhibit S1P-induced increased mote activity in store-depleted cells (Fig. 8F, Table 3). This negative result was not due to an inability of suramin to reach targets within dendrites, since we observed that it has a profound suppressive effect on synaptic transmission in these cells (data not shown, *n* = 5 cells).

We conclude that S1P most likely promotes Ca<sup>2+</sup> entry across the plasma membrane in a way that does not involve G protein-coupled receptors (GPCRs) but might instead be a direct action on a channel.

### Agents that suppress SOCE also suppress motes

Though the pharmacology of store-operated channels (SOC) varies between cells (Parekh & Putney, 2005), we would expect that some agents known to inhibit SOC opening would also suppress motes. Two inhibitors of capacitative Ca<sup>2+</sup> influx in other systems, SKF-96365 (Merritt *et al.* 1990; Bouron *et al.* 2005) and the dihydropyridine, MRS-1845 (*N*-methylnitrendipine; Harper *et al.* 2003) did not suppress motes in store-depleted cells (Table 3).

2-Aminoethoxydiphenylborane (2-APB) has been reported to have multiple pharmacological effects including suppression of SOCE (Gregory *et al.* 2001; Bilmen *et al.* 2002; Bootman *et al.* 2002; Peppiatt *et al.* 2003; Lievreumont *et al.* 2005). In chick amacrine cells, this agent is thought to act primarily as an antagonist of IP<sub>3</sub>Rs at a concentration of 50  $\mu$ M (Warrier *et al.* 2005). Consistent with this view, we saw no suppression of motes in TG-treated cells at 50  $\mu$ M (Table 3). However, as with differentiating hippocampal neurons where higher concentrations suppress SOCE (Wu *et al.* 2004), we found that 200  $\mu$ M 2-APB was effective in our cells at blocking motes in store-depleted cells and in suppressing mote induction by S1P in those cells (Fig. 9A, Table 3).

Similarly, the trivalent ion, Gd<sup>3+</sup>, which in many other systems is able to inhibit SOCE (reviewed in Smyth *et al.* 2006), was effective at suppressing motes in store-depleted cells, as well as those induced by S1P, at concentrations of

2 and 5  $\mu\text{M}$  ( $n = 10$  cells; Fig. 9B). Like the application of  $\text{La}^{3+}$  or the removal of external  $\text{Ca}^{2+}$ , we found that the effect of  $\text{Gd}^{3+}$  was rapid following its introduction into the bath.

### S1P-dependent motes accompany store emptying

For motes to be considered the expression of SOCE we would expect that treatments, other than TG, that cause

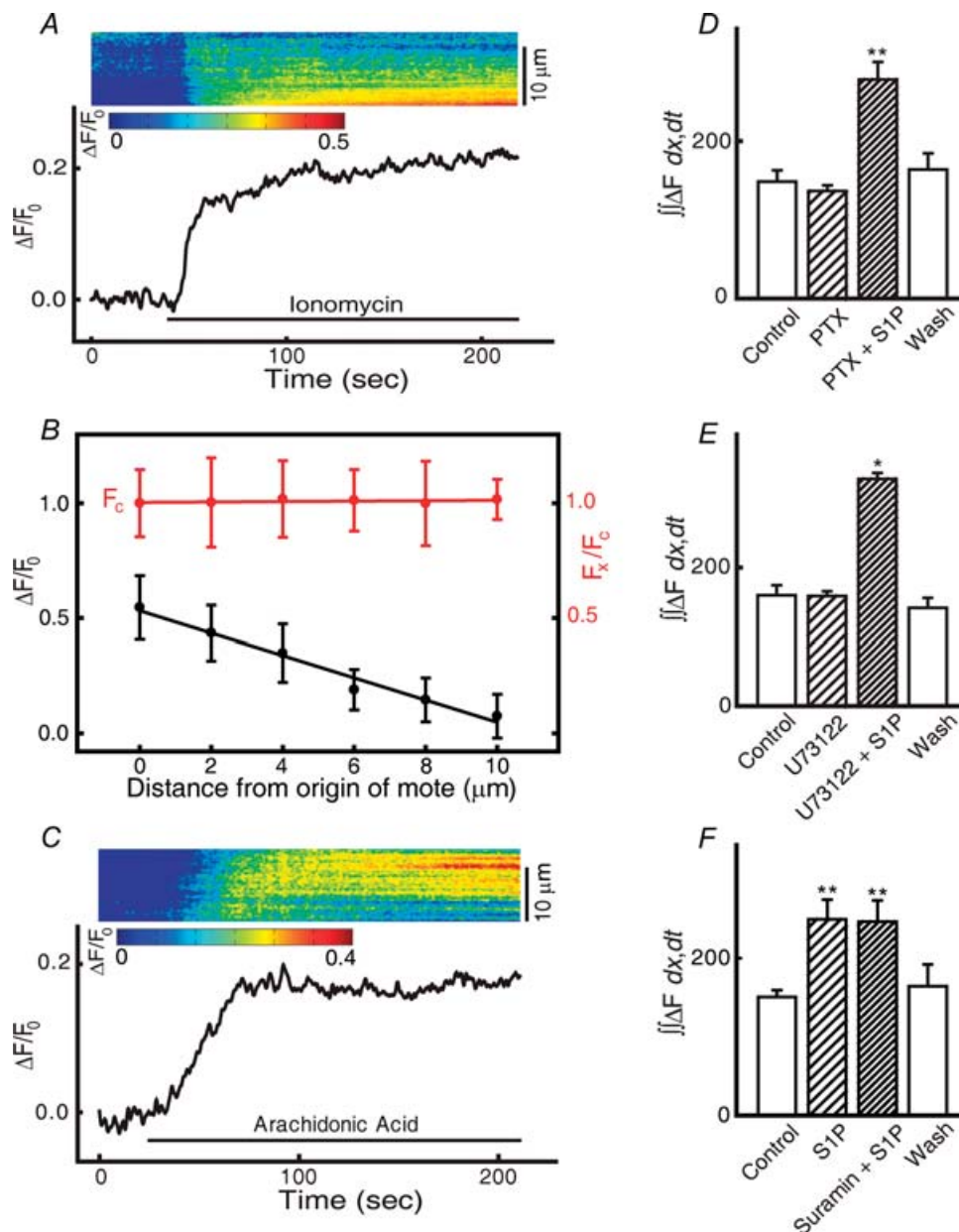


**Figure 8. S1P does not induce motes by causing a generalized increase in  $[\text{Ca}^{2+}]_i$  or activating S1P receptors**

A, a slow linescan showing that the  $\text{Ca}^{2+}$  ionophore, ionomycin (10  $\mu\text{M}$ ), applied to a store-depleted cell in normal external  $[\text{Ca}^{2+}]$  elevated  $[\text{Ca}^{2+}]_i$  but did not increase mote activity. B, the sustained rise in  $[\text{Ca}^{2+}]_i$  seen with S1P is greatest at the sites of mote origin. In 5 cells to which S1P was applied, raw fluorescence was compared at sites of mote origin and at points away from this. Before any response to S1P occurred, fluorescence values ( $F_x$ ) at all points were similar to those ( $F_c$ ) at the site of mote origin (red symbols and regression line). After  $[\text{Ca}^{2+}]_i$  had risen, but during an interval without a mote, the increase in fluorescence  $\int \Delta F/F_0$ , was examined at the same locations (black symbols). As shown by the regression line, the rise in  $[\text{Ca}^{2+}]_i$  is highest at the site of mote origin and drops to 50% at  $\sim 5.4$   $\mu\text{m}$  from this point. Error bars show s.d. C, a slow linescan showing that bath application of arachidonic acid (8  $\mu\text{M}$ ) raised  $[\text{Ca}^{2+}]_i$  but did not initiate mote activity. D, E and F, drugs likely to interfere with S1P receptor/G protein-coupled pathways were without effect on mote activity. D, pertussis toxin (1  $\mu\text{g ml}^{-1}$ , 5 cells); E, U-73122 (20  $\mu\text{M}$ , 5 cells); and F, suramin (100  $\mu\text{M}$ , 5 cells) did not inhibit or enhance mote activity nor suppress the ability of S1P to increase mote activity. \* $P \leq 0.025$ , \*\* $P \leq 0.01$ , ANOVA, Table 3.

depletion of ER  $\text{Ca}^{2+}$  stores would also trigger motes. We would expect, in addition, that these motes would be suppressed by DMS. Lastly we would predict that suppression of motes would prevent store refilling. In this and the next section we show that these expectations are fulfilled.

(*RS*)-2-chloro-5-hydroxyphenylglycine (CHPG), a ligand for metabotropic glutamate receptors, has been shown to release  $\text{Ca}^{2+}$  from internal stores via  $\text{IP}_3$  in these cells (Sosa *et al.* 2002; Warriar & Wilson, 2007). We confirmed that, as reported by Sosa *et al.* (2002), CHPG applied to the cell body of amacrine cells not previously exposed to TG, produced a large increase in  $[\text{Ca}^{2+}]_i$  due to a  $\text{Ca}^{2+}$  influx that continued after CHPG removal. When  $300 \mu\text{M}$  CHPG was puff or bath applied to dendrites, initial responses attributable to release of  $\text{Ca}^{2+}$  from internal stores were always followed by an increase in the activity of motes after a delay of variable duration (Fig. 10A). Similarly, caffeine (20 mM) when puff applied to a dendrite, elicited an immediate brief response followed by a prolonged increase in the activity of motes (Fig. 10B). Ionomycin also, when bath applied at  $50 \mu\text{M}$  in normal external  $[\text{Ca}^{2+}]$  to cells untreated with TG, invariably produced a delayed increase in mote activity (Fig. 10C), though as already shown in Fig. 8A, no increase in mote activity was seen if the stores had previously been depleted. These results demonstrate that increased mote activity is linked to the depletion of internal  $\text{Ca}^{2+}$  stores, regardless of the method by which those stores are depleted.

As expected, DMS when co-applied with any of these agents, completely suppressed motes (ionomycin + DMS,  $n = 5$  cells; caffeine + DMS,  $n = 6$  cells; CHPG + DMS,

$n = 5$  cells; Fig. 10D shows mote suppression for applied ionomycin + DMS). Similarly, when DMS was co-applied with TG in normal external  $[\text{Ca}^{2+}]$ , motes were never seen ( $n = 4$  cells), even though in the absence of DMS, as already shown (Fig. 1C), motes were plentiful. Taken together, these results provide strong evidence that S1P is a link in the chain of events connecting depletion of TG-sensitive stores with  $\text{Ca}^{2+}$  influx.

### Inhibiting motes prevents store refilling

To confirm that S1P-triggered motes are a means of replenishing  $\text{Ca}^{2+}$  stores, we employed caffeine to both deplete and subsequently interrogate  $\text{Ca}^{2+}$  stores in a protocol shown in Fig. 11A. Caffeine (20 mM in nominally 0  $[\text{Ca}^{2+}]$  external solution) was bath applied for a period of 5 min, during which the  $[\text{Ca}^{2+}]$  in dendrites rose and then fell as internal stores were depleted (Fig. 11B, inset). Caffeine was then washed out of the bath and cells were treated with either normal  $[\text{Ca}^{2+}]$  external, normal  $[\text{Ca}^{2+}]$  external plus  $5 \mu\text{M}$  DMS, or normal  $[\text{Ca}^{2+}]$  external plus DMS and  $10 \mu\text{M}$  S1P. After a 10 min recovery for refilling, the bathing solution was changed to nominally 0  $[\text{Ca}^{2+}]$  external solution for a period of 1 min to ensure complete  $\text{Ca}^{2+}$  removal. Finally, to assess the state of the internal stores, a 20 s puff of 20 mM caffeine in 0  $[\text{Ca}^{2+}]$  was applied to the dendrite and its response recorded.

After 10 min of recovery in normal external solution, internal stores had been sufficiently replenished that a robust response was elicited by the 20 s caffeine challenge. These results were quantified by measuring the peak fluorescence change immediately following the

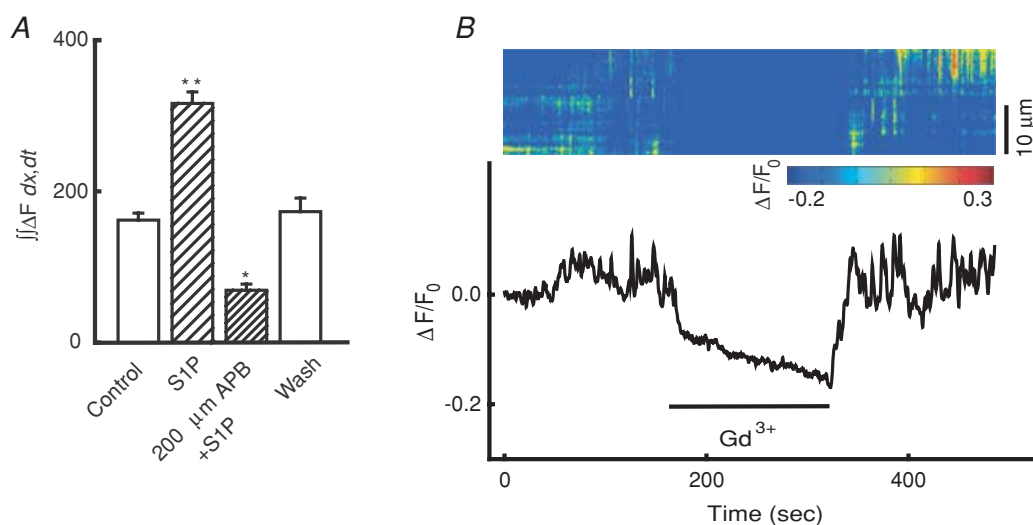


**Figure 9. Agents that suppress SOCE also suppress motes**

A,  $200 \mu\text{M}$  2-APB blocked S1P-induced motes in store-depleted cells ( $n = 5$  cells,  $*P \leq 0.025$ ,  $**P \leq 0.01$ , ANOVA, Table 3). B, a slow linescan showing that  $5 \mu\text{M}$   $\text{Gd}^{3+}$  quickly decreased  $[\text{Ca}^{2+}]_i$  and suppressed S1P-induced mote activity in a store-depleted cell.

termination of the 20 s caffeine puff. We adopted this measure instead of the usual integral of fluorescence increase because caffeine, through a direct interaction with OGB comparable to that reported for Fura-2 (Iino, 1989; Friel & Tsien, 1992), caused a small and reversible depression in fluorescence visible in many responses. When DMS ( $5 \mu\text{M}$ ) was present during recovery, responses to the caffeine challenge were significantly smaller than controls, by a factor of about 3.5. In contrast (as shown in Fig. 11B, C) in cells treated with S1P in addition to DMS, responses to the caffeine challenge were not significantly different from controls, but were significantly larger than with DMS alone.

From these results we conclude first, that during recovery in normal external solution, endogenous

production of S1P triggers motes, the  $\text{Ca}^{2+}$  influx events of SOCE in these cells, allowing the stores to refill. Second, exogenously applied DMS retards store refilling by suppressing S1P production; and third, exogenously applied S1P is sufficient to overcome the suppressive effect of DMS and allow stores to refill.

### Motes occur in resting cells

Since motes have a characteristic signature in time and space we were able to look for them in the dendrites of resting cells not exposed to TG, or any other treatment that would deplete internal  $\text{Ca}^{2+}$  stores. Surprisingly, events with the characteristics of motes were seen in about 90% of cultures. These motes were in all respects identical to those

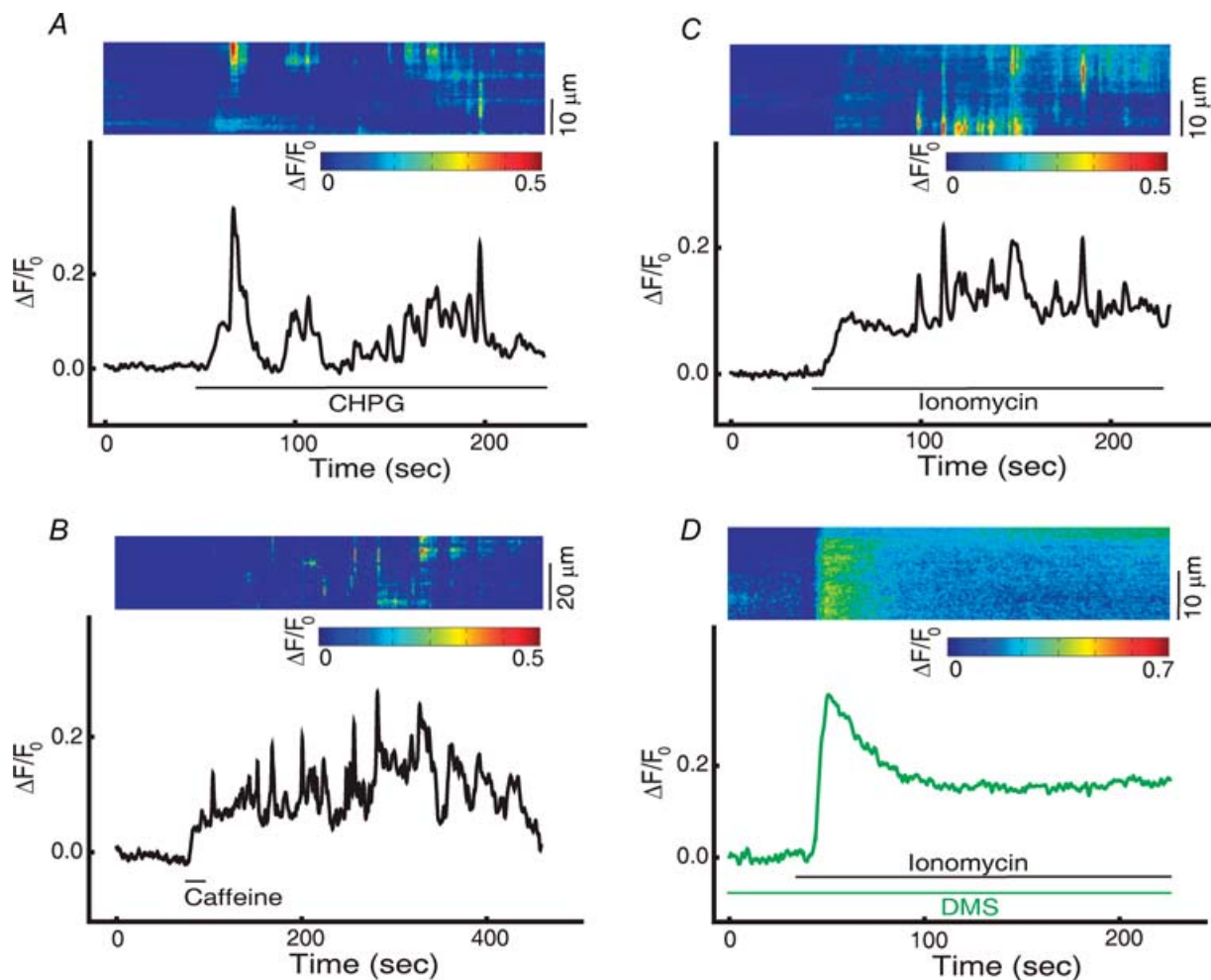


**Figure 10. In cells unexposed to TG, treatments that promote release of  $\text{Ca}^{2+}$  from internal stores also promote a prolonged increase in mote activity**

A, bath applied 300  $\mu\text{M}$  CHPG produced an initial spike of  $[\text{Ca}^{2+}]_i$ ; followed by an increase in the frequency of motes. B, puff-applied 20 mM caffeine elicited a long lasting increase in the frequency of motes following an initial rise in  $[\text{Ca}^{2+}]_i$ . This pattern was similar to that seen when caffeine was bath applied (not shown). C, ionomycin, bath applied to cells unexposed to TG in normal external  $[\text{Ca}^{2+}]_i$  solution, also induced motes following an initial rise in  $[\text{Ca}^{2+}]_i$ . D, in the presence of 7  $\mu\text{M}$  DMS, however, ionomycin failed to promote motes despite a  $[\text{Ca}^{2+}]_i$  increase.

seen after prolonged TG treatment with approximately the same average frequency of two or three per 31 s scan episode. Peak  $[Ca^{2+}]$  during these motes was  $211.9 \text{ nM}$  ( $\pm 58.0 \text{ nM}$ ,  $n = 8$  cells), not significantly different from  $197.4 \text{ nM}$  ( $\pm 49.3 \text{ nM}$ ) for those seen in store-depleted cells. In agreement with Hurtado *et al.* (2002), the resting  $[Ca^{2+}]$  in untreated cells was found to be higher than in TG-treated cells ( $74.8 \pm 15.1 \text{ nM}$ ,  $n = 6$  cells, as opposed to  $39.7 \pm 17.8 \text{ nM}$ ). From a sample of 35 events in 12 cells, we measured a mean spread of  $7.6 \mu\text{m}$  ( $\pm 3.66 \mu\text{m}$ ) and a duration of  $655 \text{ ms}$  ( $\pm 541 \text{ ms}$ ), again not significantly different from those seen after TG treatment. Like the motes seen in store-depleted cells, these were quickly

suppressed by removal of external  $Ca^{2+}$  or addition of  $La^{3+}$ , as well as addition of DMS (Table 4). As expected, we found that addition of S1P caused a significant increase in mote activity (Table 4).

## Discussion

### Motes are the expression of channel gating in the plasma membrane

Several lines of evidence show unequivocally that it is  $Ca^{2+}$  entering from the external medium that gives rise to the events we have termed 'motes'. Removal of external

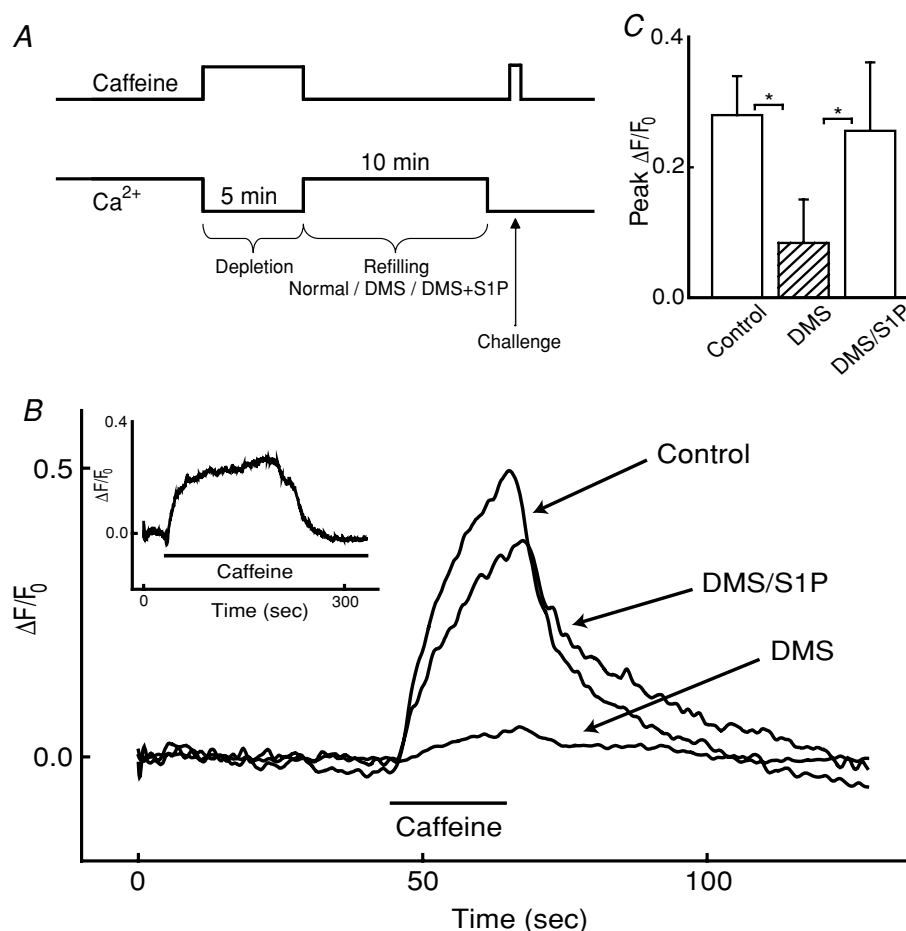


**Figure 11. Motes permit refilling of depleted  $Ca^{2+}$  stores**

A, the protocol for using caffeine to both deplete and challenge  $Ca^{2+}$  stores is illustrated here. This protocol consisted of 3 phases. Depletion: 20 mM caffeine in nominally 0  $[Ca^{2+}]$  external solution was applied for 5 min. The inset in B shows that this was sufficient to deplete the stores. Refilling: extracellular  $[Ca^{2+}]$  was returned to normal for 10 min allowing stores to refill (all cells). For DMS and DMS/S1P cells, 5  $\mu\text{M}$  DMS, or DMS and 10  $\mu\text{M}$  S1P, respectively, were also applied for the duration of this phase. Challenge: the degree of  $Ca^{2+}$  store replenishment was tested by a 20 s puff of 20 mM caffeine in 0  $[Ca^{2+}]$ . 1 min prior to this test the  $[Ca^{2+}]$  of the external solution was changed to nominally zero. B, three typical responses to the caffeine challenge are shown here. The presence of DMS during the refilling phase severely compromised store refilling, but with the addition of S1P, store refilling was restored. C, summary of data from all cells examined in this way (peak  $\Delta F/F_0$  values: control  $0.280 \pm 0.060$ ,  $n = 10$ ; DMS  $0.084 \pm 0.067$ ,  $n = 9$ ; DMS/S1P  $0.256 \pm 0.105$ ,  $n = 10$ ). A one-way rank-based ANOVA (Kruskal–Wallis), with differences evaluated using Dunn's multiple comparison procedure showed that DMS was significantly different from control and DMS/S1P ( $*P \leq 0.05$ ).



**Table 4. Effects of La<sup>3+</sup> and DMS and S1P in cells unexposed to TG**

Drug (concentration)	Mote activity $\int \int \Delta F/F_0 dx, dt$ ( $\pm$ s.d.)		
	Control	Drug	Wash
La <sup>3+</sup> (25 $\mu$ M)	170.0 $\pm$ 13.6	7.4 $\pm$ 9.3 <sup>††</sup>	178.0 $\pm$ 9.4
DMS (7 $\mu$ M)	166.3 $\pm$ 16.9	16.8 $\pm$ 6.2 <sup>†</sup>	183.7 $\pm$ 9.9
S1P (10 $\mu$ M)	164.6 $\pm$ 6.8	266.9 $\pm$ 13.1 <sup>††</sup>	166.7 $\pm$ 23.5

Statistical comparisons are relative to control.  $n = 5$  in each group.  $t$  test: <sup>††</sup> $P \leq 0.001$ , <sup>†</sup> $P \leq 0.003$ .

Ca<sup>2+</sup>, application of 25  $\mu$ M La<sup>3+</sup> or micromolar Gd<sup>3+</sup>, abolished mote activity in less than or approximately the same time required for a complete change of bathing solution. None of the conditions that induced motes, such as store emptying or the application of S1P, ever induced motes in the absence of external Ca<sup>2+</sup>, even when, as in experiments such as that shown in Fig. 1C, it was clear that internal stores were not empty.

Motes are readily seen, and can have their frequency increased, in dendrites entirely depleted of internal [Ca<sup>2+</sup>] by prolonged exposure to TG. This result stands in contrast to the ability of TG to abolish the superficially similar events (puffs and sparks) seen in other preparations, in particular, ganglion cells from the developing chick retina (Lohmann *et al.* 2002, 2005) at approximately the same developmental stage as the amacrine cells used in this study.

The channels responsible for motes are not gated by transmitters, nor are they voltage-gated or Ca<sup>2+</sup>-gated. Agonists and antagonists for the common transmitters in the retina have no effect on mote activity. Nifedipine, which is known to reduce Ca<sup>2+</sup> current and interfere with synaptic transmission in these cells (Gleason *et al.* 1994), does not affect motes, nor does voltage clamping cells at voltages below the activation range for Ca<sup>2+</sup> currents responsible for transmitter release.

The possibility that motes are the consequence of elevated [Ca<sup>2+</sup>] in the cytoplasm, as would be the case if they were mediated by Ca<sup>2+</sup>-gated cation channels for example, is ruled out by experiments on store-depleted cells in which Ca<sup>2+</sup> influx by ionomycin produced a rise in [Ca<sup>2+</sup>]<sub>i</sub> but failed to generate motes. Fortuitously, arachidonic acid was found to induce a general rise in [Ca<sup>2+</sup>]<sub>i</sub> but similarly never produced motes. While elevated [Ca<sup>2+</sup>]<sub>i</sub> does not trigger motes, there is nevertheless an association between the two phenomena. Treatments that promote motes also tend to promote a sustained elevation in [Ca<sup>2+</sup>]<sub>i</sub> at mote hotspots. Some of this sustained elevation is probably attributable to residual Ca<sup>2+</sup> from previous motes but since, as seen in Fig. 4A, for example, [Ca<sup>2+</sup>]<sub>i</sub> elevation can sometimes appear before motes, this is probably not a complete explanation. We speculate that, by analogy with Ca<sup>2+</sup> sparks in mammalian muscle (Zhou *et al.* 2003), the channels at hotspots can be

gated to generate a stereotyped mote but might also allow flickering openings.

### Sphingolipids trigger motes

Our finding that Sph, S1P and SPC all increase the activity of motes seen in dendrites, supports the idea that one or all of these sphingolipids, or perhaps a metabolic derivative, are involved in the mechanism of mote generation. The evidence suggests that S1P alone is the natural ligand. DMS, an inhibitor of the enzyme that generates S1P from Sph, entirely suppresses motes elicited by store depletion. This effect occurs, and reverses, within approximately 1 min (at 10  $\mu$ M), implying that S1P is both generated and broken down on a timescale no longer than this. Importantly, DMS suppresses the induction of motes by applied Sph, but not applied S1P. This finding has two implications. First, it implies that DMS is not acting as an antagonist directly at the Ca<sup>2+</sup> influx channel. Second, it implies that Sph must first be phosphorylated to S1P before it can act.

The inability of PTX and suramin to influence mote activity strongly suggests that S1P does not act through a G protein-linked S1P receptor but might instead work intracellularly, as it does in neutrophils (Itagaki & Hauser, 2003). If S1P is generated intracellularly, consistent with its proposed role as a step in the pathway of SOCE, it would be reasonable to assume that it acts at the intracellular face of the plasma membrane. An apparent difficulty arises then in accounting for the ability of exogenously applied S1P to also generate motes. Unlike DMS and Sph, S1P is a charged molecule and therefore unlikely to pass readily through the plasma membrane and is known not to do so in some cell types (Meyer zu Heringdorf *et al.* 2003). A possible resolution is suggested by a recent report that S1P is clearly able to cross the plasma membrane in cerebellar granule cells, by an unknown mechanism (Anelli *et al.* 2005).

### Motes represent store-operated Ca<sup>2+</sup> entry

Neurons vary in their possession of SOCE (Putney, 2003). As we show here, amacrine cells are among those that

have a distinct SOCE mechanism to refill depleted stores as argued by results both in favour of this, as well as against the alternatives.

Recent studies make it clear that in some cell types, receptor activation can trigger  $\text{Ca}^{2+}$  influx through a pathway that is pharmacologically and functionally distinct from SOCE and in parallel with it (Shuttleworth & Thompson, 1999; Luo *et al.* 2001; Mignen *et al.* 2001, 2003; Moneer & Taylor, 2002; Moneer *et al.* 2003; Holmes *et al.* 2006). Motes are unlikely to be an expression of this receptor-activated influx pathway because they can be induced by the acute application of TG, ionomycin or caffeine, all of which bypass receptor activation. Moreover, motes are suppressed by micromolar concentrations of  $\text{Gd}^{3+}$  that leave receptor-activated  $\text{Ca}^{2+}$  influx unaffected (Smyth *et al.* 2006).

Arachidonic acid, the best-described activator of this receptor pathway, is unable to induce motes at a concentration that drives the receptor-activated pathway maximally in other cells (Shuttleworth & Thompson, 1999). Further evidence against the possibility that motes represent the receptor-activated influx pathway is that OAG neither increases nor decreases the activity of motes. Nor is mote induction by S1P affected by the PLC inhibitor U-73122, strongly indicating that motes are not dependent upon the production of AA from DAG as is often the case for the receptor-activated influx pathway (Moneer & Taylor, 2002).

In practice, SOCE is defined as  $\text{Ca}^{2+}$  entry triggered by the depletion of stores with TG. In this context then, two of our findings are crucial. First, DMS suppresses the motes induced by acute application of TG, and second, suppression of motes with DMS retards refilling of caffeine-sensitive stores, an effect that can be reversed by the exogenous application of S1P. Together these experiments imply that S1P and motes are necessary for store refilling, and therefore that store depletion is coupled to the activation of sphingosine kinase. While this conclusion is in agreement with a study on neutrophils (Itagaki & Hauser, 2003), it is nevertheless unexpected since the current model of SOCE has no requirement for S1P and envisages  $\text{Ca}^{2+}$  entry promoted solely through the interaction of STIM1 in the ER membrane with a channel formed of Orai subunits in the plasmalemma (Hewavitharana *et al.* 2007). This picture may be correct for SOCE involving  $I_{\text{crac}}$ ; however, even in this instance, as pointed out by Putney (2007), the present evidence leaves room for other factors to mediate the interaction between these two membrane proteins.

Recent studies support the notion that STIM1 can both interact with and gate native SOC and some TRPC channels (Huang *et al.* 2006; Yuan *et al.* 2007), but as with the interaction of STIM1 and Orai1, no requirement for a sphingolipid has been described. There is nevertheless widespread evidence that a number of lipid molecules can

gate TRPC channels (Minke, 2006). One, TRPC5, which is expressed in cultured chick amacrine cells (E. Gleason, personal communication), has recently been reported to be directly gated by S1P (Xu *et al.* 2006b). Interestingly, TRPC5 is also thought to be activated by store depletion in arterioles (Xu *et al.* 2006a) or when heterologously expressed in HEK293 cells (Zeng *et al.* 2004). We point out however, that TRPC5 is reported not to be blocked by  $\text{Gd}^{3+}$  (Zeng *et al.* 2004), unlike the channels we describe here.

How S1P might promote  $\text{Ca}^{2+}$  entry is presently unclear but we speculate that, as has been proposed for the interaction of lysophospholipids with TRPC5 (Flemming *et al.* 2006), it might interact with membrane channels through its ability to alter the lipid environment around them. This might perhaps occur in membrane rafts (Brown & London, 2000), in which sphingolipids are an important component. There is some evidence that TRPC channels are located in rafts (Ambudkar *et al.* 2004) as well as evidence that disruption of rafts by removal of cholesterol, another raft constituent, reduces SOCE (Holmes *et al.* 2006).

Motes pose some interesting questions concerning origin of their discreteness. One mechanism that can be ruled out, however, even with the limited results we present here, is that the kinetics of motes reflect the kinetics of changes in [S1P] or the kinetics of sphingosine kinase. The finding that externally applied S1P produces motes indistinguishable from endogenous motes precludes this interpretation. By analogy with puffs and sparks it might be imagined that the calcium influx of a mote is able to close the influx channels responsible for it. For this conjecture to be true it would have to be the case that slow and relatively small changes in [ $\text{Ca}^{2+}$ ] were ineffective at closing channels since this is indicated by several pieces of evidence (see Figs 1C, 4A and 10C).

### Store replenishment occurs at special sites and occurs even in resting cells

Application of TG, which in these cells, as elsewhere, has been shown to induce emptying of ER stores, produces a much increased frequency of motes when acutely applied, though the rate seen at longer times after application is typically no greater than seen in untreated cells. This adaptation in mote frequency is consistent with SOCE (Zweifach & Lewis, 1995; Parekh, 1998; Singh *et al.* 2002) but because exogenously applied S1P is able to increase the frequency of motes in cells that have already undergone this adaptation, the site of adaptation is likely to be upstream of the channel.

One of the unexpected properties of motes is that they can typically be seen in resting cells, implying that dendrites are continually taking tiny sips of  $\text{Ca}^{2+}$  to top up

stores slowly depleted by leakage. This notion apparently runs counter to work in which SOCE is thought to occur only when internal stores are severely depleted (Mignen *et al.* 2001; Moneer & Taylor, 2002). Intrinsic differences in the systems examined might account for this, but we point out that the  $\text{Ca}^{2+}$  influx we see is small and infrequent, on the order of one mote per influx site per minute. The very small volume of dendrites enhances the visibility of motes; moreover motes would probably escape notice at the lower temporal and spatial resolutions employed in many other studies.

Our observation that S1P induces motes mostly at the same sites evident prior to its application argues that there are relatively few channels, or clusters of channels, that give rise to motes. We suggest that these sites are located so as to permit efficient refilling of the ER as is the case for CRAC channels which are concentrated at special locations where the plasma membrane and ER are juxtaposed (Luik *et al.* 2006).

## References

- Albert AP, Saleh SN, Peppiatt-Wildman CM & Large WA (2007). Multiple activation mechanisms of store-operated TRPC channels in smooth muscle cells. *J Physiol* **583**, 25–36.
- Ambudkar IS, Brazer SC, Liu X, Lockwich T & Singh B (2004). Plasma membrane localization of TRPC channels: role of caveolar lipid rafts. *Novartis Found Symp* **258**, 63–70; Discussion 70–74, 98–102, 263–106.
- Ancellin N & Hla T (1999). Differential pharmacological properties and signal transduction of the sphingosine 1-phosphate receptors EDG-1, EDG-3, and EDG-5. *J Biol Chem* **274**, 18997–19002.
- Anelli V, Bassi R, Tettamanti G, Viani P & Riboni L (2005). Extracellular release of newly synthesized sphingosine-1-phosphate by cerebellar granule cells and astrocytes. *J Neurochem* **92**, 1204–1215.
- Bilmen JG, Wootton LL, Godfrey RE, Smart OS & Michelangeli F (2002). Inhibition of SERCA  $\text{Ca}^{2+}$  pumps by 2-aminoethoxydiphenyl borate (2-APB). 2-APB reduces both  $\text{Ca}^{2+}$  binding and phosphoryl transfer from ATP, by interfering with the pathway leading to the  $\text{Ca}^{2+}$ -binding sites. *Eur J Biochem* **269**, 3678–3687.
- Bolotina VM (2004). Store-operated channels: diversity and activation mechanisms. *Sci STKE* 2004, pe34.
- Bootman MD, Collins TJ, Mackenzie L, Roderick HL, Berridge MJ & Peppiatt CM (2002). 2-aminoethoxydiphenyl borate (2-APB) is a reliable blocker of store-operated  $\text{Ca}^{2+}$  entry but an inconsistent inhibitor of  $\text{InsP}_3$ -induced  $\text{Ca}^{2+}$  release. *FASEB J* **16**, 1145–1150.
- Borges S, Gleason E, Frerking M & Wilson M (1996). Neurotensin induces calcium oscillations in cultured amacrine cells. *Vis Neurosci* **13**, 311–318.
- Bouran A, Altafaj X, Boisseau S & De Waard M (2005). A store-operated  $\text{Ca}^{2+}$  influx activated in response to the depletion of thapsigargin-sensitive  $\text{Ca}^{2+}$  stores is developmentally regulated in embryonic cortical neurons from mice. *Brain Res Dev Brain Res* **159**, 64–71.
- Brown DA & London E (2000). Structure and function of sphingolipid- and cholesterol-rich membrane rafts. *J Biol Chem* **275**, 17221–17224.
- Cheng H, Lederer MR, Xiao RP, Gomez AM, Zhou YY, Ziman B, Spurgeon H, Lakatta EG & Lederer WJ (1996). Excitation-contraction coupling in heart: new insights from  $\text{Ca}^{2+}$  sparks. *Cell Calcium* **20**, 129–140.
- Collin T, Marty A & Llano I (2005). Presynaptic calcium stores and synaptic transmission. *Curr Opin Neurobiol* **15**, 275–281.
- Connor JA, Tseng HY & Hockberger PE (1987). Depolarization- and transmitter-induced changes in intracellular  $\text{Ca}^{2+}$  of rat cerebellar granule cells in explant cultures. *J Neurosci* **7**, 1384–1400.
- Dailey ME & Smith SJ (1994). Spontaneous  $\text{Ca}^{2+}$  transients in developing hippocampal pyramidal cells. *J Neurobiol* **25**, 243–251.
- Edsall LC, Van Brocklyn JR, Cuvillier O, Kleuser B & Spiegel S (1998). N,N-Dimethylsphingosine is a potent competitive inhibitor of sphingosine kinase but not of protein kinase C: modulation of cellular levels of sphingosine 1-phosphate and ceramide. *Biochemistry* **37**, 12892–12898.
- Emptage NJ, Reid CA & Fine A (2001). Calcium stores in hippocampal synaptic boutons mediate short-term plasticity, store-operated  $\text{Ca}^{2+}$  entry, and spontaneous transmitter release. *Neuron* **29**, 197–208.
- Feske S, Gwack Y, Prakriya M, Srikanth S, Puppel SH, Tanasa B, Hogan PG, Lewis RS, Daly M & Rao A (2006). A mutation in Orai1 causes immune deficiency by abrogating CRAC channel function. *Nature* **441**, 179–185.
- Flemming PK, Dedman AM, Xu SZ, Li J, Zeng F, Naylor J, Benham CD, Bateson AN, Muraki K & Beech DJ (2006). Sensing of lysophospholipids by TRPC5 calcium channel. *J Biol Chem* **281**, 4977–4982.
- Freissmuth M, Waldhoer M, Bofill-Cardona E & Nanoff C (1999). G protein antagonists. *Trends Pharmacol Sci* **20**, 237–245.
- Friel DD & Tsien RW (1992). A caffeine- and ryanodine-sensitive  $\text{Ca}^{2+}$  store in bullfrog sympathetic neurones modulates effects of  $\text{Ca}^{2+}$  entry on  $[\text{Ca}^{2+}]_i$ . *J Physiol* **450**, 217–246.
- Galante M & Marty A (2003). Presynaptic ryanodine-sensitive calcium stores contribute to evoked neurotransmitter release at the basket cell-Purkinje cell synapse. *J Neurosci* **23**, 11229–11234.
- Gleason E, Borges S & Wilson M (1993). Synaptic transmission between pairs of retinal amacrine cells in culture. *J Neurosci* **13**, 2359–2370.
- Gleason E, Borges S & Wilson M (1994). Control of transmitter release from retinal amacrine cells by  $\text{Ca}^{2+}$  influx and efflux. *Neuron* **13**, 1109–1117.
- Gleason E & Wilson M (1989). Development of synapses between chick retinal neurons in dispersed culture. *J Comp Neurol* **287**, 213–224.
- Gregory RB, Rychkov G & Barritt GJ (2001). Evidence that 2-aminoethyl diphenylborate is a novel inhibitor of store-operated  $\text{Ca}^{2+}$  channels in liver cells, and acts through a mechanism which does not involve inositol trisphosphate receptors. *Biochem J* **354**, 285–290.

- Harper JL, Camerini-Otero CS, Li AH, Kim SA, Jacobson KA & Daly JW (2003). Dihydropyridines as inhibitors of capacitative calcium entry in leukemic HL-60 cells. *Biochem Pharmacol* **65**, 329–338.
- Hewavitharana T, Deng X, Soboloff J & Gill DL (2007). Role of STIM and Orai proteins in the store-operated calcium signaling pathway. *Cell Calcium* **42**, 173–182.
- Holmes AM, Roderick HL, McDonald F & Bootman MD (2006). Interaction between store-operated and arachidonate-activated calcium entry. *Cell Calcium* **41**, 1–12.
- Huang GN, Zeng W, Kim JY, Yuan JP, Han L, Muallem S & Worley PF (2006). STIM1 carboxyl-terminus activates native SOC,  $I_{Cracand}$  TRPC1 channels. *Nat Cell Biol* **8**, 1003–1010.
- Huba R & Hofmann HD (1990). Identification of GABAergic amacrine cell-like neurons developing in chick retinal monolayer cultures. *Neurosci Lett* **117**, 37–42.
- Hurtado J, Borges S & Wilson M (2002).  $Na^+$ - $Ca^{2+}$  exchanger controls the gain of the  $Ca^{2+}$  amplifier in the dendrites of amacrine cells. *J Neurophysiol* **88**, 2765–2777.
- Igarashi Y, Hakomori S, Toyokuni T, Dean B, Fujita S, Sugimoto M, Ogawa T, el-Ghendy K & Racker E (1989). Effect of chemically well-defined sphingosine and its N-methyl derivatives on protein kinase C and src kinase activities. *Biochemistry* **28**, 6796–6800.
- Ignatov A, Lintzel J, Kreienkamp HJ & Schaller HC (2003). Sphingosine-1-phosphate is a high-affinity ligand for the G protein-coupled receptor GPR6 from mouse and induces intracellular  $Ca^{2+}$  release by activating the sphingosine-kinase pathway. *Biochem Biophys Res Commun* **311**, 329–336.
- Iino M (1989). Calcium-induced calcium release mechanism in guinea pig taenia caeci. *J Gen Physiol* **94**, 363–383.
- Inesi G & Sagara Y (1992). Thapsigargin, a high affinity and global inhibitor of intracellular  $Ca^{2+}$  transport ATPases. *Arch Biochem Biophys* **298**, 313–317.
- Itagaki K & Hauser CJ (2003). Sphingosine 1-phosphate, a diffusible calcium influx factor mediating store-operated calcium entry. *J Biol Chem* **278**, 27540–27547.
- Khirouf L, Giniatullin R, Sokolova E, Talantova M & Nistri A (1997). Imaging of intracellular calcium during desensitization of nicotinic acetylcholine receptors of rat chromaffin cells. *Br J Pharmacol* **122**, 1323–1332.
- Koizumi S, Bootman MD, Bobanovic LK, Schell MJ, Berridge MJ & Lipp P (1999). Characterization of elementary  $Ca^{2+}$  release signals in NGF-differentiated PC12 cells and hippocampal neurons. *Neuron* **22**, 125–137.
- Lehmann N, Krishna Aradhyam G & Fahmy K (2002). Suramin affects coupling of rhodopsin to transducin. *Biophys J* **82**, 793–802.
- Lievremont JP, Bird GS & Putney JW Jr (2005). Mechanism of inhibition of TRPC cation channels by 2-aminoethoxydiphenylborane. *Mol Pharmacol* **68**, 758–762.
- Liou J, Kim ML, Heo WD, Jones JT, Myers JW, Ferrell JE Jr & Meyer T (2005). STIM is a  $Ca^{2+}$  sensor essential for  $Ca^{2+}$ -store-depletion-triggered  $Ca^{2+}$  influx. *Curr Biol* **15**, 1235–1241.
- Llano I, Gonzalez J, Caputo C, Lai FA, Blayney LM, Tan YP & Marty A (2000). Presynaptic calcium stores underlie large-amplitude miniature IPSCs and spontaneous calcium transients. *Nat Neurosci* **3**, 1256–1265.
- Lohmann C, Finski A & Bonhoeffer T (2005). Local calcium transients regulate the spontaneous motility of dendritic filopodia. *Nat Neurosci* **8**, 305–312.
- Lohmann C, Myhr KL & Wong RO (2002). Transmitter-evoked local calcium release stabilizes developing dendrites. *Nature* **418**, 177–181.
- Lohmann C & Wong RO (2005). Regulation of dendritic growth and plasticity by local and global calcium dynamics. *Cell Calcium* **37**, 403–409.
- Luik RM, Wu MM, Buchanan J & Lewis RS (2006). The elementary unit of store-operated  $Ca^{2+}$  entry: local activation of CRAC channels by STIM1 at ER-plasma membrane junctions. *J Cell Biol* **174**, 815–825.
- Luo D, Broad LM, Bird GS & Putney JW Jr (2001). Mutual antagonism of calcium entry by capacitative and arachidonic acid-mediated calcium entry pathways. *J Biol Chem* **276**, 20186–20189.
- Merritt JE, Armstrong WP, Benham CD, Hallam TJ, Jacob R, Jaxa-Chamiec A, Leigh BK, McCarthy SA, Moores KE & Rink TJ (1990). SK&F 96365, a novel inhibitor of receptor-mediated calcium entry. *Biochem J* **271**, 515–522.
- Meyer zu Heringdorf D, Liliom K, Schaefer M, Danneberg K, Jaggar JH, Tigyi G & Jakobs KH (2003). Photolysis of intracellular caged sphingosine-1-phosphate causes  $Ca^{2+}$  mobilization independently of G-protein-coupled receptors. *FEBS Lett* **554**, 443–449.
- Mignen O, Thompson JL & Shuttleworth TJ (2001). Reciprocal regulation of capacitative and arachidonate-regulated noncapacitative  $Ca^{2+}$  entry pathways. *J Biol Chem* **276**, 35676–35683.
- Mignen O, Thompson JL & Shuttleworth TJ (2003).  $Ca^{2+}$  selectivity and fatty acid specificity of the noncapacitative, arachidonate-regulated  $Ca^{2+}$  (ARC) channels. *J Biol Chem* **278**, 10174–10181.
- Minke B (2006). TRP channels and  $Ca^{2+}$  signaling. *Cell Calcium* **40**, 261–275.
- Moneer Z, Dyer JL & Taylor CW (2003). Nitric oxide co-ordinates the activities of the capacitative and non-capacitative  $Ca^{2+}$ -entry pathways regulated by vasopressin. *Biochem J* **370**, 439–448.
- Moneer Z & Taylor CW (2002). Reciprocal regulation of capacitative and non-capacitative  $Ca^{2+}$  entry in A7r5 vascular smooth muscle cells: only the latter operates during receptor activation. *Biochem J* **362**, 13–21.
- Niedernberg A, Tunaru S, Blaukat A, Ardati A & Kostenis E (2003). Sphingosine 1-phosphate and dioleoylphosphatidic acid are low affinity agonists for the orphan receptor GPR63. *Cell Signal* **15**, 435–446.
- Parekh AB (1998). Slow feedback inhibition of calcium release-activated calcium current by calcium entry. *J Biol Chem* **273**, 14925–14932.
- Parekh AB & Putney JW Jr (2005). Store-operated calcium channels. *Physiol Rev* **85**, 757–810.
- Peppiatt CM, Collins TJ, Mackenzie L, Conway SJ, Holmes AB, Bootman MD, Berridge MJ, Seo JT & Roderick HL (2003). 2-Aminoethoxydiphenyl borate (2-APB) antagonises inositol 1,4,5-trisphosphate-induced calcium release, inhibits calcium pumps and has a use-dependent and slowly reversible action on store-operated calcium entry channels. *Cell Calcium* **34**, 97–108.

- Prakriya M, Feske S, Gwack Y, Srikanth S, Rao A & Hogan PG (2006). Orai1 is an essential pore subunit of the CRAC channel. *Nature* **443**, 230–233.
- Putney JW Jr (1986). A model for receptor-regulated calcium entry. *Cell Calcium* **7**, 1–12.
- Putney JW Jr (2003). Capacitative calcium entry in the nervous system. *Cell Calcium* **34**, 339–344.
- Putney JW Jr (2007). New molecular players in capacitative  $\text{Ca}^{2+}$  entry. *J Cell Sci* **120**, 1959–1965.
- Reichling DB & MacDermott AB (1993). Brief calcium transients evoked by glutamate receptor agonists in rat dorsal horn neurons: fast kinetics and mechanisms. *J Physiol* **469**, 67–88.
- Roos J, DiGregorio PJ, Yeromin AV, Ohlsen K, Lioudyno M, Zhang S, Safrina O, Kozak JA, Wagner SL, Cahalan MD, Velicelebi G & Stauderman KA (2005). STIM1, an essential and conserved component of store-operated  $\text{Ca}^{2+}$  channel function. *J Cell Biol* **169**, 435–445.
- Sagara Y, Fernandez-Belda F, de Meis L & Inesi G (1992). Characterization of the inhibition of intracellular  $\text{Ca}^{2+}$  transport ATPases by thapsigargin. *J Biol Chem* **267**, 12606–12613.
- Sanchez T & Hla T (2004). Structural and functional characteristics of S1P receptors. *J Cell Biochem* **92**, 913–922.
- Segal M (1993). GABA induces a unique rise of  $[\text{Ca}]_i$  in cultured rat hippocampal neurons. *Hippocampus* **3**, 229–238.
- Shuttleworth TJ & Thompson JL (1999). Discriminating between capacitative and arachidonate-activated  $\text{Ca}^{2+}$  entry pathways in HEK293 cells. *J Biol Chem* **274**, 31174–31178.
- Singh BB, Liu X, Tang J, Zhu MX & Ambudkar IS (2002). Calmodulin regulates  $\text{Ca}^{2+}$ -dependent feedback inhibition of store-operated  $\text{Ca}^{2+}$  influx by interaction with a site in the C terminus of TrpC1. *Mol Cell* **9**, 739–750.
- Smyth JT, Dehaven WI, Jones BF, Mercer JC, Trebak M, Vazquez G & Putney JW Jr (2006). Emerging perspectives in store-operated  $\text{Ca}^{2+}$  entry: Roles of Orai, Stim and TRP. *Biochim Biophys Acta* **1763**, 1147–1160.
- Sosa R & Gleason E (2004). Activation of mGluR5 modulates  $\text{Ca}^{2+}$  currents in retinal amacrine cells from the chick. *Vis Neurosci* **21**, 807–816.
- Sosa R, Hoffpauir B, Rankin ML, Bruch RC & Gleason EL (2002). Metabotropic glutamate receptor 5 and calcium signaling in retinal amacrine cells. *J Neurochem* **81**, 973–983.
- Spiegel S & Milstien S (2000). Functions of a new family of sphingosine-1-phosphate receptors. *Biochim Biophys Acta* **1484**, 107–116.
- Sun XP, Callamaras N, Marchant JS & Parker I (1998). A continuum of  $\text{InsP}_3$ -mediated elementary  $\text{Ca}^{2+}$  signalling events in *Xenopus* oocytes. *J Physiol* **509**, 67–80.
- Suryanarayanan A & Slaughter MM (2006). Synaptic transmission mediated by internal calcium stores in rod photoreceptors. *J Neurosci* **26**, 1759–1766.
- Takemura H, Hughes AR, Thastrup O & Putney JW Jr (1989). Activation of calcium entry by the tumor promoter thapsigargin in parotid acinar cells. Evidence that an intracellular calcium pool and not an inositol phosphate regulates calcium fluxes at the plasma membrane. *J Biol Chem* **264**, 12266–12271.
- Thastrup O, Cullen PJ, Drobak BK, Hanley MR & Dawson AP (1990). Thapsigargin, a tumor promoter, discharges intracellular  $\text{Ca}^{2+}$  stores by specific inhibition of the endoplasmic reticulum  $\text{Ca}^{2+}$ -ATPase. *Proc Natl Acad Sci U S A* **87**, 2466–2470.
- Toman RE & Spiegel S (2002). Lysophospholipid receptors in the nervous system. *Neurochem Res* **27**, 619–627.
- Tsien RY (1989). Fluorescent probes of cell signaling. *Annu Rev Neurosci* **12**, 227–253.
- Uhlenbrock K, Gassenhuber H & Kostenis E (2002). Sphingosine 1-phosphate is a ligand of the human gpr3, gpr6 and gpr12 family of constitutively active G protein-coupled receptors. *Cell Signal* **14**, 941–953.
- van Koppen C, Meyer zu Heringdorf M, Laser KT, Zhang C, Jakobs KH, Bunemann M & Pott L (1996). Activation of a high affinity  $\text{G}_i$  protein-coupled plasma membrane receptor by sphingosine-1-phosphate. *J Biol Chem* **271**, 2082–2087.
- Vig M, Peinelt C, Beck A, Koomoa DL, Rabah D, Koblan-Huberson M, Kraft S, Turner H, Fleig A, Penner R & Kinet JP (2006). CRACM1 is a plasma membrane protein essential for store-operated  $\text{Ca}^{2+}$  entry. *Science* **312**, 1220–1223.
- Warrier A, Borges S, Dalcino D, Walters C & Wilson M (2005). Calcium from internal stores triggers GABA release from retinal amacrine cells. *J Neurophysiol* **94**, 4196–4208.
- Warrier A & Wilson M (2007). Endocannabinoid signaling regulates spontaneous transmitter release from embryonic retinal amacrine cells. *Vis Neurosci* **24**, 25–35.
- Wu X, Zagranichnaya TK, Gurda GT, Eves EM & Villereal ML (2004). A TRPC1/TRPC3-mediated increase in store-operated calcium entry is required for differentiation of H19-7 hippocampal neuronal cells. *J Biol Chem* **279**, 43392–43402.
- Xu SZ, Boulay G, Flemming R & Beech DJ (2006a). E3-targeted anti-TRPC5 antibody inhibits store-operated calcium entry in freshly isolated pial arterioles. *Am J Physiol Heart Circ Physiol* **291**, H2653–H2659.
- Xu SZ, Muraki K, Zeng F, Li J, Sukumar P, Shah S, Dedman AM, Flemming PK, McHugh D, Naylor J, Cheong A, Bateson AN, Munsch CM, Porter KE & Beech DJ (2006b). A sphingosine-1-phosphate-activated calcium channel controlling vascular smooth muscle cell motility. *Circ Res* **98**, 1381–1389.
- Yang L, Yatomi Y, Satoh K, Igarashi Y & Ozaki Y (1999). Sphingosine 1-phosphate formation and intracellular  $\text{Ca}^{2+}$  mobilization in human platelets: evaluation with sphingosine kinase inhibitors. *J Biochem (Tokyo)* **126**, 84–89.
- Yao Y, Choi J & Parker I (1995). Quantal puffs of intracellular  $\text{Ca}^{2+}$  evoked by inositol trisphosphate in *Xenopus* oocytes. *J Physiol* **482**, 533–553.
- Yatomi Y, Ruan F, Megidish T, Toyokuni T, Hakomori S & Igarashi Y (1996). N,N-dimethylsphingosine inhibition of sphingosine kinase and sphingosine 1-phosphate activity in human platelets. *Biochemistry* **35**, 626–633.
- Yeromin AV, Zhang SL & Jiang W, Yu Y, Safrina O & Cahalan MD (2006). Molecular identification of the CRAC channel by altered ion selectivity in a mutant of Orai. *Nature* **443**, 226–229.

- Yuan JP, Zeng W, Huang GN, Worley PF & Muallem S (2007). STIM1 heteromultimerizes TRPC channels to determine their function as store-operated channels. *Nat Cell Biol* **9**, 636–645.
- Zeng F, Xu SZ, Jackson PK, McHugh D, Kumar B, Fountain SJ & Beech DJ (2004). Human TRPC5 channel activated by a multiplicity of signals in a single cell. *J Physiol* **559**, 739–750.
- Zhou J, Brum G, Gonzalez A, Launikonis BS, Stern MD & Rios E (2003). Ca<sup>2+</sup> sparks and embers of mammalian muscle. Properties of the sources. *J Gen Physiol* **122**, 95–114.
- Zweifach A & Lewis RS (1995). Slow calcium-dependent inactivation of depletion-activated calcium current. Store-dependent and -independent mechanisms. *J Biol Chem* **270**, 14445–14451.

### Acknowledgements

We thank Eric Leaver for useful discussions during this work and Evanna Gleason, Pam Pappone and Roger Hardie for commenting on the manuscript. This work was supported by National Eye Institute Grants EY04112 and EY12576.